THESIS FOR THE DEGREE OF DOCTOR OF PHILOSOPHY

On cyclic accumulation models for degradation of railway foundations

Using experimental design in geotechnical FE modelling

HOSSEIN TAHERSHAMSI

Department of Architecture and Civil Engineering
Division of Geology and Geotechnics
CHALMERS UNIVERSITY OF TECHNOLOGY

Gothenburg, Sweden 2023

On cyclic accumulation models for degradation of railway foundations
Using experimental design in geotechnical FE modelling
HOSSEIN TAHERSHAMSI
ISBN 978-91-7905-810-4

Doktorsavhandlingar vid Chalmers tekniska högskola
Ny serie nr. 5276
ISSN 0346-718X
Department of Architecture and Civil Engineering
Division of Geology and Geotechnics
Chalmers University of Technology
SE-412 96 Gothenburg
Sweden
Telephone: +46 (0)31-772 1000

Cover:
Longitudinal cross section of a conventional railway system

Chalmers Reproservice
Gothenburg, Sweden 2023

On cyclic accumulation models for degradation of railway foundations
Using experimental design in geotechnical FE modelling
Thesis for the degree of Doctor of Philosophy
HOSSEIN TAHERSHAMSI
Department of Architecture and Civil Engineering
Division of Geology and Geotechnics
Chalmers University of Technology

ABSTRACT

The degradation of railway foundations due to the repeated loading of traffic induces maintenance and safety obligations for the track operator. One major contributor to track degradation is the accelerated settlement rates in soft soils below the track that lead to alignment issues, especially at stiffness transitions. Furthermore, due to the low stiffness of most soft soils, significant ground vibrations are emitted and lead to low critical train velocities that avoid track resonance. In addition, the dynamic properties of the soil, particularly weakly bonded soft natural clays, are subject to significant alternations over the lifetime of the railway structure due to cyclic traffic loading. The soil/foundation is thus a major source of degradation issues that, as opposed to track and subgrade-related causes, are largely controlled by local site conditions.

This thesis aims at identifying a proper sensitivity analysis method in geotechnical Finite Element Analysis (FEA) for optimal use of advanced constitutive soil models. For this purpose, first the viscoplastic Creep-SCLAY1S model is evaluated for a boundary value problem. The objective was ultimately addressed by implementing two Global Sensitivity Analysis (GSA) methods for quantifying the uncertainties of Creep-SCLAY1S. The common GSA method of Sobol was benchmarked against Experimental design in a lab-scale numerical model of Constant Rate of Strain (CRS). The Sobol method has proven to be computationally expensive for sensitivity analysis of advanced constitutive models using FEA. The spatial sensitivity measures of Sobol and Experimental design indicate that they are not altogether distinct. Thus, Experimental design represents a more feasible approach by using less resources, such as computational time and required storage. Furthermore, temporal Sensitivity Analysis (SA) has demonstrated the importance of the entire time domain spectrum, particularly for factor fixing purposes.

The second part of the study proposes a revised strain accumulation model that has been validated using new data on Swedish natural clay for cyclic loads with low amplitude. The model presented herein offers a strong basis for the accurate prediction of strain accumulation in soft clays beneath embankments subjected to a significant number of loading cycles. In general, the knowledge gained in this research contributes to a better understanding of comprehensive numerical models in Geotechnics and can be a helpful prior to inverse modelling, data assimilation, and Random Finite Element Method (RFEM).

Keywords: Cyclic degradation, Natural soft clay, Uncertainty analysis, Cyclic accumulation models, Global Sensitivity Analysis, Experimental design, Sobol method, Rate-dependent models

to my dear parents.

PREFACE

The research presented in this thesis was conducted at the Division of Geology and Geotechnics, Chalmers University of Technology, spanning from September 2017 to April 2023. The author is grateful to the Swedish Transport Administration for financing this project within the framework of BIG (Branch samverkan i Grund).

I extend my sincere gratitude to my supervisor, Prof. Jelke Dijkstra, for his invaluable guidance, support, and motivation throughout my research journey. I am also thankful to my examiner, Prof. Minna Karstunen, for her constructive feedback and comments on this study, which helped me to improve the quality of my work. I will always hold them in the highest regard for their contributions.

I would also like to acknowledge the support of Mikael Öhman, Mats Karlsson and Georgios Birmpilis for their assistance in different aspects of my research. Filip Nilenius deserves special thanks for teaching me experimental design, which has greatly influenced and inspired this research. My gratitude also goes to my colleagues at the Geotechnical Research Group for their kindness and support.

My deepest love and appreciation go to my wonderful family, who have been my constant source of support and motivation. I would like to express my gratitude to my exceptional mother for being so awesome and considerate. To my dear sister Leila, your incredible achievements and passion for research have inspired me beyond words. A special thank you to my brother Mohammad and his family for their assistance during my days in Sweden. Finally, to my beloved father, I am forever grateful for your unwavering guidance, advice, suggestions, and encouragement. Thank you for all your support throughout this journey.

Gothenburg, Sweden 2023
Hossein Tahershamsi

NOTATION

Acronyms

CRS: Constant Rate of Strain
CSS: Current Stress Surface
DOE: Design of Experiments
FD: Factorial Design
FE: Finite Element
FEM: Finite Element Method
FF: Factor Fixing
FP: Factor Prioritisation
GDS: Global Digital Systems
GSA: Global Sensitivity Analysis
ICS: Intrinsic Compression Surface
LVDT: Linear Variable Differential Transducers
NCS: Normal Consolidation Surface
OCR: Over-consolidation ratio
OFAT: One-Factor-At-a-Time
RFEM: Random Finite Element Method
SA: Sensitivity Analysis

Greek letters

α_0 initial inclination of NCS
χ_0 initial amount of bonding
$\dot{\Gamma}$ Revised cyclic viscoplastic multiplier
$\dot{\Lambda}$ rate-dependent viscoplastic multiplier
$\dot{\Omega}$ Creep-SCLAY1Sc cyclic viscoplastic multiplier
ϵ_d^c viscoplastic deviatoric strain
ϵ_d^e elastic deviatoric strain
ϵ_v^c viscoplastic volumetric strain
ϵ_v^e elastic volumetric strain
κ^* modified swelling index
λ_i^* modified intrinsic compression index
μ_i^* intrinsic modified creep index
ν Poisson's ratio
ω absolute effectiveness of rotational hardening
ω_d relative effectiveness of rotational hardening
ψ Scaling parameter related to amplitude dependency
ρ_b bulk density
σ'_{p_0} initial pre-consolidation pressure
τ reference time
θ modified Lode angel
ϖ small-strain multiplier

Roman lower case letters

a absolute rate of destructuration
b relative rate of destructuration
k number of input factors
m_ϵ strain resistance number
p' mean effective stress
p'_{eq} equivalent mean effective stress
p'_p mean effective preconsolidation pressure
q deviatoric stress
q_{cyc} cyclic deviatoric stress
q_m superimposed deviatoric stress
q_p pre-shearing deviatoric stress
r_{si} intrinsic creep number
s_u undrained shear strength
w_N natural water content

Miscellaneous

$\langle \bullet \rangle$ Macaulay brackets

Roman capital letters

$\mathbf{C}$ contrast matrix

$\mathbf{E}$	vector of effects
$\mathbf{R}$	response vector
A	shape factor for small-strain stiffness
B	small-strain parameter related to unload/reload
G	shear modulus
M_c	slope of critical state line in triaxial compression
M_e	slope of the critical state line in triaxial extension
N	Monte Carlo sample size, number of cycles
R	resistance
R_ϵ	strain resistance
S_i	Sobol's first-order index
S_T	Sobol's total-order index
S_t	clay's sensitivity
T	loading period

THESIS

This thesis consists of an extended summary and a collection of appended papers. The computational aspects of the research, including implementation, coding and creation of illustrations, were all carried out by the author, who also wrote the initial drafts of all the papers in full. In case of Paper C, the laboratory tests were conducted by Reza Ahmadi Naghadeh, a PostDoc, with the subsequent interpretation and model development performed by the PhD candidate.

Paper A H. Tahershamsi and J. Dijkstra (2021). "Towards rigorous boundary value level sensitivity analyses using FEM". in: *IOP Conference Series: Earth and Environmental Science* 710.1, p. 012072. DOI: 10.1088/1755-1315/710/1/012072. URL: https://doi.org/10.1088/1755-1315/710/1/012072

Paper B H. Tahershamsi and J. Dijkstra (2022). "Using experimental design to assess rate-dependent numerical models". In: *Soils and Foundations* 62.6, p. 101244. ISSN: 0038-0806. DOI: https://doi.org/10.1016/j.sandf.2022.101244

Paper C H. Tahershamsi, R. Ahmadi Naghadeh, B. Zuada Coelho, and J. Dijkstra (2023). "Low amplitude strain accumulation model for natural soft clays below railways". In: *Submitted to Transportation Geotechnics*

OTHER PUBLICATIONS BY THE AUTHOR

- Dijkstra, J. and Tahershamsi, H. (2020a). *Dynamic response of a transition zone on soft clay*. Tech. rep. Chalmers University of Technology, Sweden.
- Dijkstra, J. and Tahershamsi, H. (2020b). *Modelling deformations below high-speed rail*. Tech. rep. Chalmers University of Technology, Sweden.
- Dijkstra, J., Tahershamsi, H., and Ahmadi-Naghadeh, R. (2022). *Degradation of a natural sensitive clay under cyclic loading*. Tech. rep. Chalmers University of Technology, Sweden.

CONTENTS

Part I
Extended summary

1 Introduction

1.1 Background

Degradation mechanisms in railway structures are a matter of concern to railway infrastructure administrations in terms of maintenance and safety. This is especially the case for countries with well-developed, yet ageing, networks where large parts are founded on soft soils. The excessive maintenance of alignment in the track systems requires large investments by the general public. Predictive maintenance strategies rely on the ability to foresee the need for maintenance early before substantial issues arise. Thus, a clear comprehension of the sources of degradation mechanisms and their associated prediction tools for railway systems are required.

During operation of the railway system, degradation occurs gradually over the long-term in the foundation system that comprises the ballast, subballast and subgrade. The subgrade includes the embankment, the sub-soil below and any additional structural foundation elements. Railway embankments on natural soft clays, which is the focus of this research, were typically built many decades ago with only limited amount of reinforcements, whereas modern foundations incorporate piled embankments or other ground improvement methods. Soft clay exhibits several intriguing features, such as sensitivity, anisotropy, and rate-dependency, underpinning the complexity of its non-linear and time-dependent response under hydro-mechanical loading (Mitchell and Soga, 2005). Some of this complexity has been generalised in constitutive models for subsequent numerical analyses to predict the behaviour of soft clays with sufficient accuracy (*e.g.* Wheeler et al., 2003; Karstunen et al., 2005; Dafalias et al., 2006; Gras et al., 2018). Cyclic degradation in soft soils is a complex phenomenon that incorporates many factors to model (*e.g.* Zuada Coelho et al., 2021; Staubach et al., 2022). Modelling is highly preferable as a means of assessing and predicting the behaviour of existing railway structures over the long term, as measurements are time-consuming, expensive and non-predictive. Thus, it is required to develop models to accurately capture the behaviour of soft soil beneath railway embankments under typical low-amplitude cyclic loading.

In order to make reliable predictions using numerical models, they need to be calibrated against laboratory data and ultimately validated against field data. Due to the uncertainties and increasing complexity of numerical models, calibration processes may become non-unique (Gras et al., 2017). The behaviour of such models, nevertheless needs to be evaluated, and the cost of the experimental design and calibration processes should be optimised before application to real-world engineering. Hence, a systematic statistical approach for the assessment of numerical models is required, particularly for predicting the rate-dependent and cyclic response of soft soils. Such approaches allow scrutinising the impact of different model components and their associated parameters, in addition to the quantification of uncertainties (Box, Hunter, et al., 2009). Furthermore, there is a need to understand model uncertainties throughout the spatial and temporal domain of boundary value problems; hence, a spatial sensitivity analysis that evolves in time is also necessary to capture

the most reliable information for subsequent model calibration and numerical analyses at field scale.

1.2 Aims and objectives

The project aims to investigate the feasibility of using advanced sensitivity analysis methods for the quantification of a permissible pseudo-static and dynamic response of railway systems on soft clays. In the first part, the aim is to determine a feasible technique for Global Sensitivity Analysis (GSA) with which the uncertainties of Finite Element-based numerical models in transportation geotechnics are quantified. In the second part, a revised strain accumulation model for cyclic loads with low amplitude is proposed and validated against new data on Swedish natural clay. Considering the overall aim of this research study, the following objectives are defined:

- Implement promising Global Sensitivity Analysis (GSA) methods for boundary value problems.
- Evaluate the most suitable GSA method for geotechnical analyses.
- Benchmark the GSA methods regarding sensitivity measures, accuracy, computational costs, and the amount of information they provide.
- Evaluate rate-dependent models for creep and cyclic strain accumulation in soft soils.
- Revise an existing rate-dependent model for creep and cyclic strain accumulation in soft clays to represent the clay response under low amplitude cyclic loading, as relevant for railways, based on new data on cyclic degradation on natural Swedish clay.

1.3 Limitations

The limitations of this study are summarised as below:

- Primarily idealised numerical examples are used throughout the sensitivity analysis of the models.
- Only a limited number of constitutive models, suitable for modelling the rate-dependent response of soft sensitive clays under quasi-static and cyclic loading, will be considered.

2 Literature review

2.1 Degradation of railway systems: a brief geotechnical overview

The majority of research on cyclic foundation response has emerged from offshore engineering problems, where Ultimate Limit State (ULS) governs the design. In such designs, the structure can tolerate substantial uniform settlements but occasionally, limited differential settlements are permissible (Randolph and Gourvenec, 2017). As a result, the ULS approach, which focuses on stability, is more prevalent than the design for Serviceability Limit State (SLS) for dimensioning offshore and onshore foundations under cyclic loads (*e.g.* Andersen, 2009).

A commonly used ULS approach involves generalising cyclic data from laboratory tests performed under undrained conditions with relatively large loading amplitudes into stability diagrams (Andersen, 1988). These stability design layouts depict the relationship between the number of cycles required for failure and the average shear stress and cyclic shear stress using contour diagrams. Such diagrams provide valuable insights into the interplay between these factors and help to identify the approximate capacity of geostructure under cyclic loading. Based on the findings of Sangrey et al. (1969) and Ansal and Erken (1989), a threshold stress ratio was established using laboratory tests in which no failure occurs because of cyclic loading. Furthermore, even for cyclic loads below the critical stress ratio that do not induce soil failure, ongoing deformations occur, albeit at a smaller magnitude (*e.g.* Zhao, J. Liu, et al., 2023). In contrast, a few approaches have been developed to investigate the long-term Serviceability Limit State (SLS) response, *i.e.* differential settlements and vibrations of railway foundations under cyclic loading with moderate loading amplitude (*e.g.* Bian et al., 2014; Cui et al., 2015; Zhao, J. Liu, et al., 2023).

Alignment issues of linear infrastructure, especially railways, have attracted substantial attention over the past decades (Indraratna, Ionescu, et al., 1998; Augustin et al., 2003; Guler et al., 2011; X. Li et al., 2016; Nielsen and X. Li, 2018). The degradation in railways may stem from the reduction of bearing capacity and accumulated deformations in the track system and subsoil due to long-term cyclic loading. This mechanism occasionally leads to uneven settlements; thus, the alignment and longitudinal level of the railway track is affected (Esveld, 2001).

The components of a conventional railway system, in general, consist of a substructure and a superstructure. The rails, the fastening system, and the sleepers form the superstructure; whereas the elements of the substructure are ballast, subballast and subgrade (Selig and Waters, 1994). The vast majority of studies are designed towards the behaviour and deterioration of the ballast or subballast layers in railway systems (Indraratna and Salim, 2002; Suiker and Borst, 2003; Salim and Indraratna, 2004; Suiker, Selig, et al., 2005; Indraratna, Thakur, et al., 2012). Thus, the response of the foundation/soil in the substructure has been ignored to a great extent. For instance, excessive levels of vibration were observed in a railway embankment located at Ledsgård, Sweden. These vibrations were primarily attributed to the existence of soft natural clay in the subsoil foundation (Krylov et al., 2000). Moreover, the investigation findings also revealed substantial settlements in multiple locations, especially over soft natural soils (Holm et al., 2002).

The combined dynamic response of the subsoil and railway system for a single train passage has been studied and modelled by several authors (*e.g.* Madshus and Kaynia, 2000; Hall, 2003; Alves Costa et al., 2010). Subsequently, more rigorous studies have been conducted using non-linear soil models, including Woodward et al. (2015) and Shih et al. (2017). In these studies,

the significance of models that capture non-linear elastic stiffness and irreversible degradation of the shear modulus in soft soils is highlighted. Nevertheless, few studies have been focusing on the long-term Serviceability Limit State of railway systems on soft natural clays, including irreversible deformations. The long-term response of cyclically loaded foundations on soft soils has been investigated, by means of a viscoplastic cyclic accumulation model by Zuada Coelho et al. (2021). The response of the proposed model agreed well with laboratory data, with relatively large loading amplitudes, both at element level and boundary value problems. Furthermore, the model capability was demonstrated for a hypothetical case of an embankment on soft soil.

2.2 Rate-dependency of natural clays

The long-term behaviour of soft clays has shown that deformation continues after dissipation of excess porewater pressures, *i.e.* consolidation in the sample finishes (Buisman, 1936). In addition to the primary consolidation, a second time-dependent mechanism is identified while $\sigma' =$ constant, *i.e.* secondary consolidation (pure creep). The two phases are in reality overlapping; however, Janbu (1985) showed that in some engineering cases, the hydrodynamic process vanishes relatively soon after load application; thus, pure creep behaviour governs the settlement process in some soft soils.

The time effects of soft clays at low loading rates, in which the time scale of load application is substantially less than the time scale of flow, have been investigated by several authors (*e.g.* Sällfors, 1975; Tavenas, Leroueil, et al., 1978; Graham et al., 1983; Leroueil et al., 1985). Sällfors (1975) demonstrated the effects of strain rate on the apparent pre-consolidation pressures and critical shear stress by means of Constant Rate of Strain (CRS) tests. Shrinkage of the size of yield surfaces have been captured in soft clays under lower rates of loading or longer application of the permanent load. This contraction of yield *locus* leads to a reduction of apparent pre-consolidation pressure and shear strength (Tavenas and Leroueil, 1977; Tavenas, Leroueil, et al., 1978; Graham et al., 1983).

In addition to evidence of creep in clays, Mitchell (1964) showed the impact of the clay structure on rate dependency at low loading rates. Thus, the creep rates in remoulded samples of natural clay are significantly lower than the intact natural samples, as shown for Swedish clays (*e.g.* Karlsson et al., 2016; Y. Li et al., 2018). The porewater pressure is another factor that influences the rate dependency of natural clays, especially in undrained and partially drained loading paths. Concerning Constant Rate of Strain (CRS) tests, Muir Wood (2016) indicated the importance of system-level interpretation of laboratory tests due to non-uniformity of excess porewater pressures at larger strain levels.

The importance of strain rate effects in numerical modelling of embankments on soft natural soils has been emphasised by many authors (*e.g.* Rowe and Hinchberger, 1998; Yildiz and Uysal, 2016). A summary of the main points involves risk of creep failure, stability problems both during and after construction, in addition to prediction accuracy of long term settlements. As a result, several constitutive models have been developed that include rate dependency, associated with other features (anisotropy, destructuration) that control the response of soft natural clays (*e.g.* Grimstad et al., 2010; Yin et al., 2010; Sivasithamparam, Karstunen, et al., 2015; Gras et al., 2018).

2.3 Cyclic response of natural clays

The cyclic response of soft clays is often investigated for undrained loading paths in the laboratory, as this is the condition that mostly reflects the practical situation (*e.g.* Janbu, 1985; Lefebvre and LeBoeuf, 1987). Janbu (1985) remarked on the necessity of interpreting effective stress for a rational explanation of the cyclic response. This interpretation highlights the role of inter-particle interactions (soil skeleton) in mobilising shear stresses, not the free water, air voids or both. Therefore, the stress dependency of the model should be built upon the effective stress concept.

The information regarding both excess porewater pressures and vertical strains can be quantified as a function of load repetition numbers N for saturated clay under cyclic loading during undrained conditions. Janbu (1985) found the uncanny resemblance of cyclic response with creep formulae, highlighted in his Rankine Lecture, by realising the proportionality of cumulative irreversible strain with either time t or number of cycles N [†]. This idea will be further formalised in terms of a constitutive model in Section 3.1.3.1.

Systematic cyclic data on natural clays are scarce, in comparison to monotonic testing of soft sensitive clays. Lefebvre and LeBoeuf (1987) conducted a few cyclic CIUC triaxial tests and subsequently compared those to monotonic tests. The cyclic tests have been performed either at a strain-controlled condition with an axial strain rate of $1\,\%\,\mathrm{h}^{-1}$ or stress-controlled at a frequency of 0.1 Hz. A small porewater pressure generation was observed for intact samples under cyclic loading. In contrast, however, large excess porewater pressures were generated for remoulded samples, *i.e.* sufficiently large to bring the test to failure for that particular loading path.

A limited amount of experimental data on the behaviour of soft natural clay is available, in which the impact of loading frequency and loading amplitude are investigated (L.-L. Li et al., 2011; Wichtmann et al., 2013). A soil specimen subjected to undrained cyclic loading with a constant cyclic shear stress q_{cy} is shown in Fig. 2.1, in which q_0 is the initial consolidation shear stress and q_a represents the average shear stress.

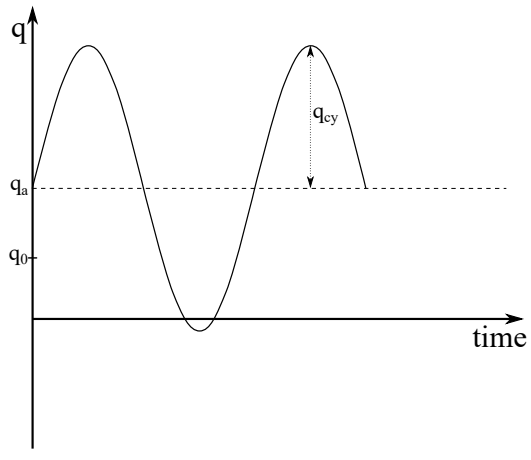

Figure 2.1: *Cyclic and average shear stresses (Andersen, 2009)*

[†] $t = NT$, in which T is the period of cycles

Natural sensitive clays show three main features as observed from cyclic undrained triaxial tests performed on block samples of soft Norwegian clay (Wichtmann et al., 2013):

(i) Fig. 2.2 indicates the existence of a semi-logarithmic relation between axial strain ε_a and the number of cycles N until the onset of failure.

(ii) At fixed loading amplitudes, the failure has occurred in a smaller number of cycles due to a lower loading frequency f; see Fig. 2.2a.

(iii) At fixed loading frequencies, failure has occurred in a smaller number of cycles due to the application of a higher cyclic shear stress amplitude $q_{\mathrm{cy,\,i}}$; see Fig. 2.2b.

Two sources of failure have been noticed in the tests: i) the observation that samples with small average shear stress shows a large shear strain amplitude accumulating during the first few cycles towards failure when tested under stress control. ii) In contrast, samples with higher average shear stresses are only brought to failure after an excessive accumulation of permanent irreversible strains.

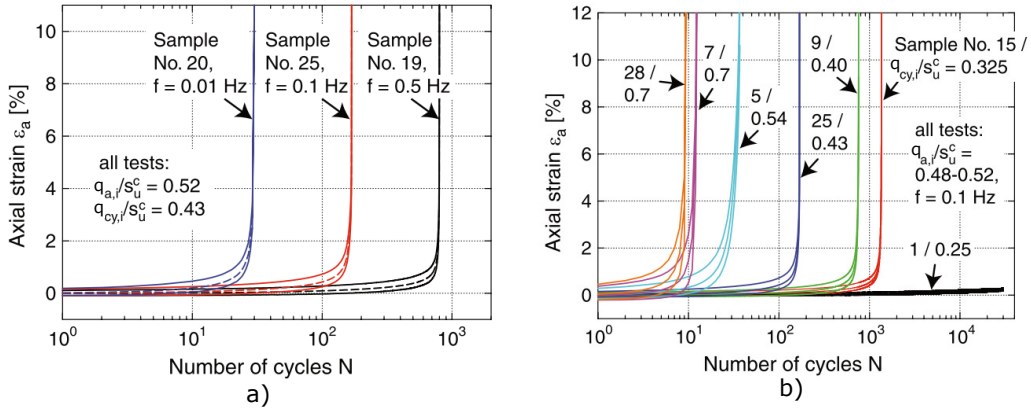

Figure 2.2: *a) Effect of loading frequency f b) effects of cyclic shear loading amplitude $q_{cy,i}$, i.e. normalised with undrained shear strength s_u^c from monotonic tests (Wichtmann et al., 2013).*

2.4 The stiffness at small strains

Natural clays, in particular when overconsolidated, may exhibit high initial stiffness at small strain when sheared or compressed. There will be a noticeable reduction in stiffness when the yield *locus* is reached. Meanwhile, the stiffness will attenuate gradually as the stress path approaches the yield surface. Burland (1989) reports several examples from London clay that shows the non-linear elasticity with high stiffness at axial strains of less than about 0.1 %. Jardine et al. (1986) have demonstrated the significance of non-linear elasticity throughout different practical examples, such as excavation, piling and footing. A family of empirical degradation curves is proposed by several authors (*e.g.* Hardin and Drnevich, 1972; Darendeli, 2001).

The interpretation of laboratory tests in conjunction with field measurements are made easier by considering the impacts of non-linear elasticity, particularly for soil-structure interaction problems. In sensitive clays that are slightly overconsolidated (OCR < 2), a similar reduction in stiffness with increasing strain magnitude is observed, as such Wood (2016) investigated the response of Swedish soft clays.

2.5 Rate-dependent constitutive models for sensitive clays

A version of a constitutive model for soft clays that originated from the Modified Cam Clay (MCC) model by Roscoe and Burland (1968) is described briefly in the following. The constitutive model has been refined in its predictive accuracy by hierarchically introducing additional model features. Following the anisotropic behaviour observed in natural clays , *i.e.* captured for drained stress probing of Otaniemi clay in triaxial tests, the anisotropic elastoplastic model SCLAY1 was first proposed (Wheeler et al., 2003). Since soft natural clay exhibits rate-dependent (creep) behaviour, Sivasithamparam, Karstunen, et al. (2015) reformulated the SCLAY1 model to include rate effects. Inspired by the work of Karstunen et al. (2005), the Creep-SCLAY1S model included the structure-related features of SCLAY1S, in addition to anisotropy and rate-dependency (Gras et al., 2018). The schematic evolution of the Creep-SCLAY1S is shown in Fig. 2.3.

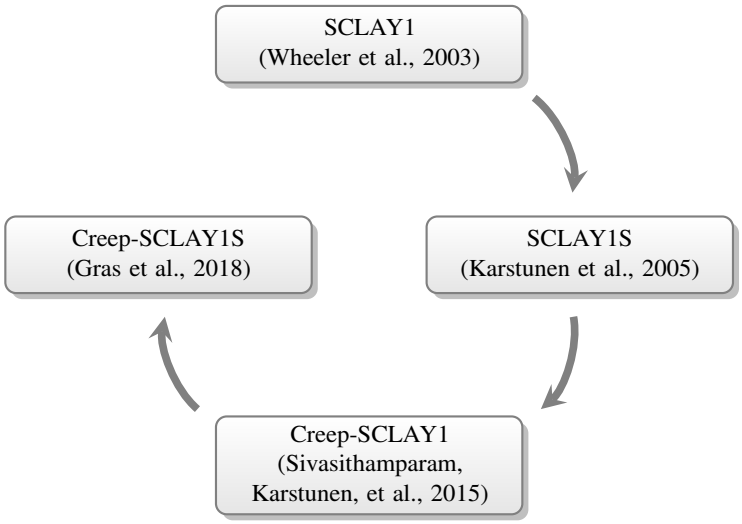

Figure 2.3: *Evolution of SCLAY1 critical state model.*

2.5.1 Creep-SCLAY1S

In the Creep-SCLAY1S model, anisotropy is described by rotating all surfaces that respectively correspond to the intrinsic, current stress and normal compression states. In the following, the model is described in the simplified case of a triaxial stress state. The shape and orientation of all surfaces are similar and defined according to Eq. (2.1):

$$f_{\text{surface}} = \left(q - \alpha p'\right)^2 - \left(M\left(\theta\right)^2 - \alpha^2\right)\left(p'_{\text{surface}} - p'\right)p' = 0 \tag{2.1}$$

The anisotropy scalar α defines the orientation of these surfaces. M, the stress ratio at a critical state is consequently a function of the modified Lode angle θ given by Eq. (2.2):

$$M(\theta) = M_c\left(\frac{2m^4}{1 + m^4 + \left(1 - m^4\right)\sin 3\theta_\alpha}\right)^{\frac{1}{4}}, \qquad \text{where} \quad m = \frac{M_e}{M_c} \tag{2.2}$$

In Eq. (2.2), M_c and M_e are the slopes of the critical state lines in triaxial compression and extension, respectively.

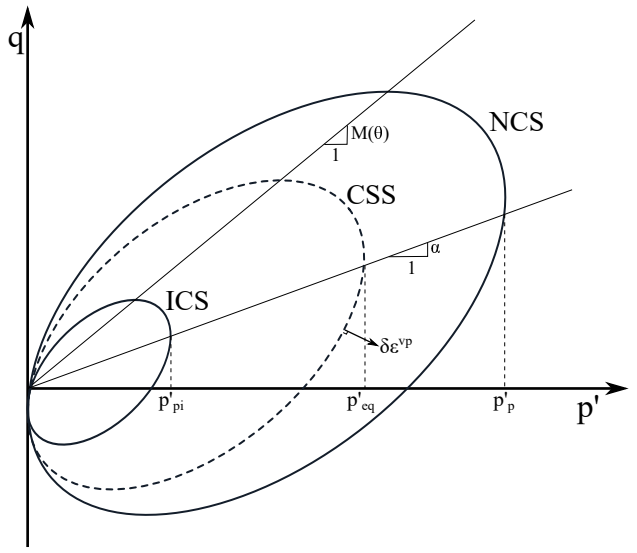

Figure 2.4: *Creep-SCLAY1S yield surfaces (Gras et al., 2018)*

Following Sivasithamparam, Karstunen, et al. (2015) and Gras et al. (2018), each reference surface captures a specific state shown in Fig. 2.4:

- Normal Consolidation Surface (NCS): A boundary surface between the small and large creep strains. Thus, there are elastic and viscoplastic strains at all times. The size of this surface is determined by the vertical pre-consolidation pressure projected on the isotropic axis p'_p.
- Current Stress Surface (CSS): This surface tracks the current state of effective stress. While loading, with a stress path moving the CSS towards NCS, the viscoplastic strains gradually become more significant. When the stress path crosses the NCS perimeter, large creep strains will develop. The size of CSS is determined by the hydrostatic mean effective stress p'_{eq} corresponding to the current effective stress state.
- Intrinsic Compression Surface (ICS): This state represents an (imaginary) soil sample without bonding, but with a similar void ratio and fabric of the NCS surface. The intrinsic

isotropic pre-consolidation pressure p'_{pi} defines the size of this imaginary surface. The size of ICS and NCS are linked together by a bonding parameter χ given in Eq. (2.3).

$$p'_p = (1 + \chi)p'_{pi} \tag{2.3}$$

The viscoplastic strains are irreversible similar to the plastic strains in an elasto-plastic model. Total strain rates are given by the summation of elastic and viscoplastic (creep) strain rates:

$$\begin{aligned} \dot{\epsilon_v} &= \dot{\epsilon_v^e} + \dot{\epsilon_v^c} \\ \dot{\epsilon_d} &= \dot{\epsilon_d^e} + \dot{\epsilon_d^c} \end{aligned} \tag{2.4}$$

In Eq. (2.4), $\dot{\epsilon^c}$ and $\dot{\epsilon^e}$ are the creep and elastic components of the total strain rate, respectively. $\dot{\epsilon_v}$ denotes the volumetric strain, whereas $\dot{\epsilon_d}$ is the deviatoric component. The creep strains in Eq. (2.4) are defined using the associated flow rule:

$$\begin{aligned} \dot{\epsilon_v^c} &= \dot{\Lambda}\frac{\partial p'_{eq}}{\partial p'} \\ \dot{\epsilon_d^c} &= \dot{\Lambda}\frac{\partial p'_{eq}}{\partial q} \end{aligned} \tag{2.5}$$

In Eq. (2.5), $\dot{\Lambda}$ is the constant rate of the visco-plastic multiplier (Sivasithamparam, Karstunen, et al., 2015):

$$\dot{\Lambda} = \frac{\mu_i^*}{\tau}\left(\frac{p'_{eq}}{p'_p}\right)^{\beta}\left(\frac{M(\theta)^2 - \alpha^2_{K_0^{nc}}}{M(\theta)^2 - \eta^2_{K_0^{nc}}}\right) \tag{2.6}$$

In Eq. (2.6), μ_i^* is the modified intrinsic creep index taken from the secondary slope of $(\ln t : \epsilon_v)$ for a reconstituted soil in which the entire structure has been remoulded (Gras et al., 2017). τ denotes the reference time, corresponding to the duration of the load step in the oedometer test from which the preconsolidation pressure has been derived. For instance, if the pre-consolidation pressure is derived from a standard oedometer test loaded with 24 hour load steps, the reference time is set to one day.

β is the ratio given in Eq. (2.7):

$$\beta = \frac{\lambda_i^* - \kappa^*}{\mu_i^*} \tag{2.7}$$

$\alpha_{K_0^{nc}}$ is the inclination of surfaces in the normally consolidated state, $\eta_{K_0^{nc}}$ is the stress ratio corresponding to a soil in its normally consolidated state; K_0^{nc}.

Creep-SCLAY1S has three hardening laws:

- *Volumetric hardening law*: The rate of the viscoplastic volumetric strain governs the size of the ICS; see Eq. (2.8):

$$\dot{p'_p} = \frac{p'_{pi}}{\lambda_i^* - \kappa^*}\dot{\epsilon_v^c} \tag{2.8}$$

- *Rotational hardening law*: Initially proposed by Wheeler et al. (2003), the rotational hardening law captures the evolving anisotropy by incorporating the rate of the volumetric viscoplastic strain $\dot{\epsilon}_v^{c\ddagger}$ and the deviatoric viscoplastic strain $\dot{\epsilon}_d^c$ according to Eq. (2.9).

$$\dot{\alpha} = \omega \left[\left(\frac{3q}{4p'} - \alpha \right) \left\langle \dot{\epsilon}_v^c \right\rangle + \omega_d \left(\frac{q}{3p'} - \alpha \right) \left| \dot{\epsilon}_d^c \right| \right] \tag{2.9}$$

- *Destructuration hardening law*: Eq. (2.10) incorporates the degradation of the fabric structure by introducing two additional parameters, *i.e.* the absolute and relative rate of destructuration (a&b). In this assumption, both the volumetric and deviatoric viscoplastic strains tend to decrease the bonding parameter χ until it totally vanishes to zero, *i.e.* an irreversible degradation of the initial bonding (Karstunen et al., 2005).

$$\dot{\chi} = -a\chi \left(\left| \dot{\epsilon}_v^c \right| + b \left| \dot{\epsilon}_d^c \right| \right) \tag{2.10}$$

Succinctly, the Creep-SCLAY1S model has 15 model parameters of which four are used to initialise the state variables. The input parameters and their description has been tabulated in Table 2.1.

Table 2.1: Description of Creep-SCLAY1S model parameters

Feature	Parameter	Unit	Description
Isotropic	κ^*	–	Modified swelling index
	ν'	–	Poisson's ratio
	λ_i^*	–	Modified intrinsic compression index
	M_c	–	Slope of critical state line in triaxial compression
	M_e	–	Slope of the critical state line in triaxial extension
Anisotropic	ω	–	Absolute effectiveness of rotational hardening
	ω_d	–	Relative effectiveness of rotational hardening
	α_0 †	–	Initial inclination of the reference surface
Structure	a	–	Absolute rate of destructuration
	b	–	Relative rate of destructuration
	χ_0 †	–	Initial amount of bonding
Viscous	τ	d	Creep reference time
	μ_i^*	–	Intrinsic modified creep index
Initial conditions	OCR †	–	Over-consolidation ratio
	e_0 †	–	Initial void ratio

† Initial state variables

‡The symbols $\langle\rangle$ are Macaulay brackets which describe a ramp function for the volumetric viscoplastic strain:

$$\left\langle \dot{\epsilon}_v^c \right\rangle = \begin{cases} \dot{\epsilon}_v^c, & \dot{\epsilon}_v^c \geq 0 \\ 0, & \dot{\epsilon}_v^c < 0 \end{cases}$$

2.6 Modelling the cyclic accumulation of soils

The accumulated strain is the irreversible component that emerges during a loading cycle in which the corresponding stress loop is completed. Thus, some permanent strain remains and the material does not return to its initial configuration. Following the conventional approach, the complete loading history is calculated with the help of a stress-strain constitutive model containing different constitutive relations and hardening laws that capture the evolving incremental stiffness. Niemunis et al. (2005) and Wichtmann (2005) have classified such an approach as *implicit* and have highlighted its inefficiency for modelling a large number of cycles, as the computational burden increases. Moreover, some numerical errors accumulate during the integration of each step since no constitutive model is free from systematic error (Niemunis et al., 2005).

An alternative concept, *i.e.* referred to as the *explicit* approach, is based on capturing the long-term deformations due to a large number of cycles. Examples and applications of explicit models are found in the research of Suiker and Borst (2003), Niemunis et al. (2005), François et al. (2010), Pasten et al. (2014), Zuada Coelho et al. (2021), and Staubach et al. (2022). With the exception of Zuada Coelho et al. (2021) and Staubach et al. (2022), in which an accumulation model is proposed for clays, most studies have been focusing on coarse grained materials.

Suiker and Borst (2003) developed a cyclic accumulation model for granular material subjected to large amplitudes of cyclic loading. The constitutive relations were developed for coarse grained materials aimed at capturing the volumetric compaction and frictional sliding mechanisms resulting from cyclic loading. Their model response has been calibrated against laboratory results on ballast and subgrade materials and compared to measurements of a railway track. The findings revealed that the actual response of the course granular substructure is influenced by various factors including the magnitude of the applied stress level, the stress path and the cyclic loading period. François et al. (2010) formulated an accumulation model for granular materials subjected to low cyclic loading amplitudes. Similar to other accumulation models, their methodology splits the modelling into an implicit part (fully described loading cycle) of which the subsequent stress will be used in the explicit part to generate accumulated strain. As a result, in the implicit part, the soil-structure response due to a single load passage is calculated and the long-term behaviour of the soil-structure is modelled according to the explicit strain-accumulation law.

In the current study, the concept of strain accumulation is used to explicitly model the deformations resulting from the cyclic loading of soils.

2.6.1 Creep-SCLAY1Sc

The Creep-SCLAY1Sc model is an extension of Creep-SCLAY1S, *i.e.* developed for cyclic loading by Zuada Coelho et al. (2021). It incorporates the accumulation of irreversible strain from cyclic loading as an additional component of viscoplastic strain using a second cumulative viscoplastic multiplier. Therefore, the proposed model can be considered to be an explicit model for cyclic loading that captures the long-term response of natural clays.

The constitutive model follows a similar strain decomposition as Eq. (2.4), except for the inclusion of a cyclic component in the viscoplastic strain tensor, with the following result:

$$\dot{\boldsymbol{\epsilon}} = \dot{\boldsymbol{\epsilon}}^{e} + \underbrace{(\dot{\boldsymbol{\epsilon}}^{c} + \dot{\boldsymbol{\epsilon}}^{cyc})}_{\dot{\boldsymbol{\epsilon}}^{vp}} \tag{2.11}$$

where in Eq. (3.25):

$\dot{\epsilon}^{e}$ = elastic strain rate
$\dot{\epsilon}^{vp}$ = viscoplastic strain rate
$\dot{\epsilon}^{c}$ = creep strain rate
$\dot{\epsilon}^{cyc}$ = cyclic strain rate

The associated flow rule remains the same as in Eq. (2.5), however with an additional viscoplastic multiplier $\dot{\Omega}$ that captures the cyclic accumulation. Thus, the viscoplastic component of Eq. (3.25) becomes:

$$\dot{\epsilon}^{vp} = [\dot{\Omega} + \dot{\Lambda}]\frac{\partial p'_{eq}}{\partial \boldsymbol{\sigma}'} \tag{2.12}$$

The cyclic viscoplastic multiplier is based on the observed behaviour of Onsøy clay under undrained triaxial loading at different loading amplitudes and periods (Wichtmann et al., 2013). The proposed Eq. (2.13) contains three normalised terms: term *i* represents the gradient of the cyclic axial strain (comparable to the μ_i^* in Eq. (2.6)); term *ii* controls the frequency dependency of the model; and term *iii* captures the loading amplitude dependence.

$$\dot{\Omega} = \underbrace{\frac{\zeta}{t_{\text{ref}|0.1\%}}}_{i}\underbrace{\left(\frac{T}{T_0}\right)^{\Xi}}_{ii}\underbrace{\left(\frac{q_{\text{cyc}}}{p'M(\theta) - q}\right)^{\iota}}_{iii} \tag{2.13}$$

and $t_{\text{ref}|0.1\%}$, *i.e.* the cyclic reference time at 0.1% of deviatoric strain, is defined in Eq. (2.14):

$$t_{\text{ref}|0.1\%} = \Gamma_{\alpha}\left(\frac{q_{\text{cyc}}}{p'_0}\right)^{-\Gamma_{\beta}} \tag{2.14}$$

T_0 and T in Eq. (2.13) denote the reference and current loading period, respectively. q_{cyc} is the cyclic deviatoric stress, $M(\theta)$ the critical state stress ratio, p' the current mean effective stress, and q the current deviatoric stress. Moreover, p'_0 stated in Eq. (2.14) is the initial mean effective stress. In conclusion, the cyclic viscoplastic multiplier introduces five more parameters in which:

- ζ: Axial strain accumulation factor in [d]; controls the gradient of the cyclic strain (*i.e.* measured at reference time $t_{\text{ref}|0.1\%}$)
- Γ_{α}: scaling factor of cyclic reference time
- Γ_{β}: exponential scaling factor of cyclic reference time
- Ξ: scaling factor of loading period
- ι: scaling factor for the fraction of cyclic and static loading

2.7 Statistical approaches

The sources of uncertainty in Geotechnical Engineering stem from the heterogeneity of soils. Tang et al. (1976) classify the sources of uncertainty into three main categories: inherent variability, measurement errors, and transformation (model) uncertainty. The variability of soils, in general, is inherited from the geological, geo-environmental, and anthropogenic processes on both spatial and temporal scales. The measurement errors are caused by the differences between the hydro-mechanical properties derived from laboratory tests and *in-situ* conditions and can have many sources, including sample disturbance, test procedures and limitations in equipment. The empirical or mathematical models that are defined based on such data inherit an inevitable source of uncertainty, *i.e.* denoted as transformation uncertainty (Phoon and Kulhawy, 1999a). Due to the existence of such uncertainties, a flexible design approach is required to match actual geotechnical field conditions.

The Observational Method, as opposed to conventional predefined design processes, is valuable for dealing with uncertainties linked to ground conditions found during construction (Peck, 1969). The originality of the Observational Method lies in the additional information gained from performance monitoring during the construction stage. The knowledge associated with the actual response under field conditions results in the reduction of uncertainty and risk (Masurier et al., 2006). The study by Spross and Johansson (2017) provides a probabilistic optimisation methodology for the Observational Method by defining a reliability constraint. In contrast to conventional exploration techniques used in Engineering Geology, Einstein and Baecher (1983) demonstrated the advantages of utilising statistical methods in subsurface exploration. A common approach to dealing with the sources of uncertainty is to employ probabilistic methods. Several researchers have quantified geotechnical uncertainties as part of reliability-based methods for geotechnical designs using probabilistic approaches (*e.g.* Tang et al., 1976; Phoon and Kulhawy, 1999a,b).

Due to the spatial variability in geomaterials, the associated span in measured properties of the material is relatively large. The spatial heterogeneities can be rigorously incorporated in numerical analyses using random fields (Fenton and Vanmarcke, 1990). In this approach, random fields are used for each model parameter or state variable in the numerical model rather than considering a mean (constant) value of the full domain. This approach was implemented in the Finite Element Method, so-called RFEM, to effectively model the impact of spatial heterogeneities on the response of several geostructures in Geotechnical Engineering (*e.g.* Fenton and Griffiths, 1993; Griffiths and Fenton, 1993; Fenton and Griffiths, 2002). Uncertainties from transformation errors in the numerical model are not explicitly considered in RFEM. Furthermore, for very complex models, it is not trivial to identify the most important model parameters that need to be considered in RFEM.

Sensitivity Analysis (SA) is highly advantageous for model evaluation and decision-making purposes (Phoon, 2020). Since the advanced constitutive models used in Geotechnics consist of many input parameteers, the computational cost of conducting probabilistic analyses involving all factors increases dramatically. By employing a systematic SA technique, the insignificant factors to the response changes can be distinguished; therefore, the computational burden decreases by fixing those in subsequent analyses. Furthermore, it is possible to quantify the dependency of the factors using a proper SA method (Saltelli, Ratto, et al., 2008; Box, Hunter, et al., 2009). For relevant literature on using SA methods in Geotechnical Engineering, see such authors as Miro et al. (2014), Khaledi et al. (2016), W. Liu et al. (2017), Zhao, Lavasan, et al. (2018), Mahmoudi

et al. (2019), and Fang and Su (2020).

3 Methodology

In the following, a brief review of the Global Sensitivity Analysis (GSA) methods used in part 1 of this thesis will be elaborated. Part 2 consists of two sections, *i.e.* the implementation of GSA methods for two laboratory tests that are evaluated at a boundary value level. In Part 3, a revised strain accumulation model together with small-strain stiffness formulation is presented. Fig. 3.1 describes an overview of the different parts of the thesis.

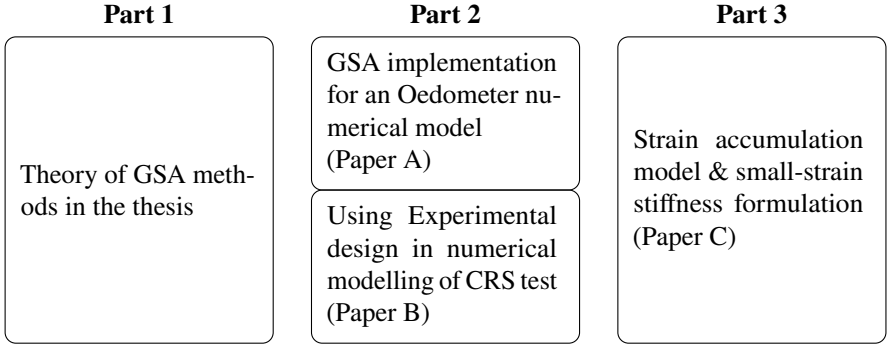

Figure 3.1: *Overview of methodology within three parts.*

Since the author has employed statistical methods in Geotechnical Engineering, it is necessary to define some statistical terms that might otherwise confuse a geotechnical reader. A common approach to performing Sensitivity Analysis (SA) in Engineering disciplines often involves changing One Factor At a Time (OFAT) while keeping others fixed. Practising engineers tend to strongly favour OFAT due to their long-standing familiarity with it, making it challenging to convince them to adopt other optimal approaches (Czitrom, 1999).

In the event more practical techniques are required, Global Sensitivity Analysis (GSA) methods offer the best trade-off between efficiency and non-linearity of models. The term *Global Sensitivity Analysis* refers to specific SA techniques that explore the entire range of input factors within a plausible domain. Some examples of GSA methods include the variance-based method of Sobol, the Elementary Effects method, and Experimental design (Saltelli and Annoni, 2010). An *experiment* refers to the operation of a system with k input factors adjusted to some definite set of levels. When investigating a process or system, such as a geotechnical FE model, the special arrangement of points chosen to study a model response relationship is called an *Experimental design* (Box and Draper, 1987). Thus, the reader should be careful not to confuse *Experimental design* with geotechnical tests that are carried out either in a laboratory or in the field.

In this thesis, GSA methods are applied to FE analysis of geotechnical problems in order to gain a comprehensive understanding of model behaviour at a system level. The significance of GSA application can be recognised either from the inception of geotechnical projects or during the construction stage as presented in Fig. 3.2.

More specifically, the implementation of the prominent Sobol method is addressed in Paper A. The implementation is demonstrated in conjunction with Creep-SCLAY1S for an incremental loading oedometer test case. The results showed the benefits of using GSA methods in assessing

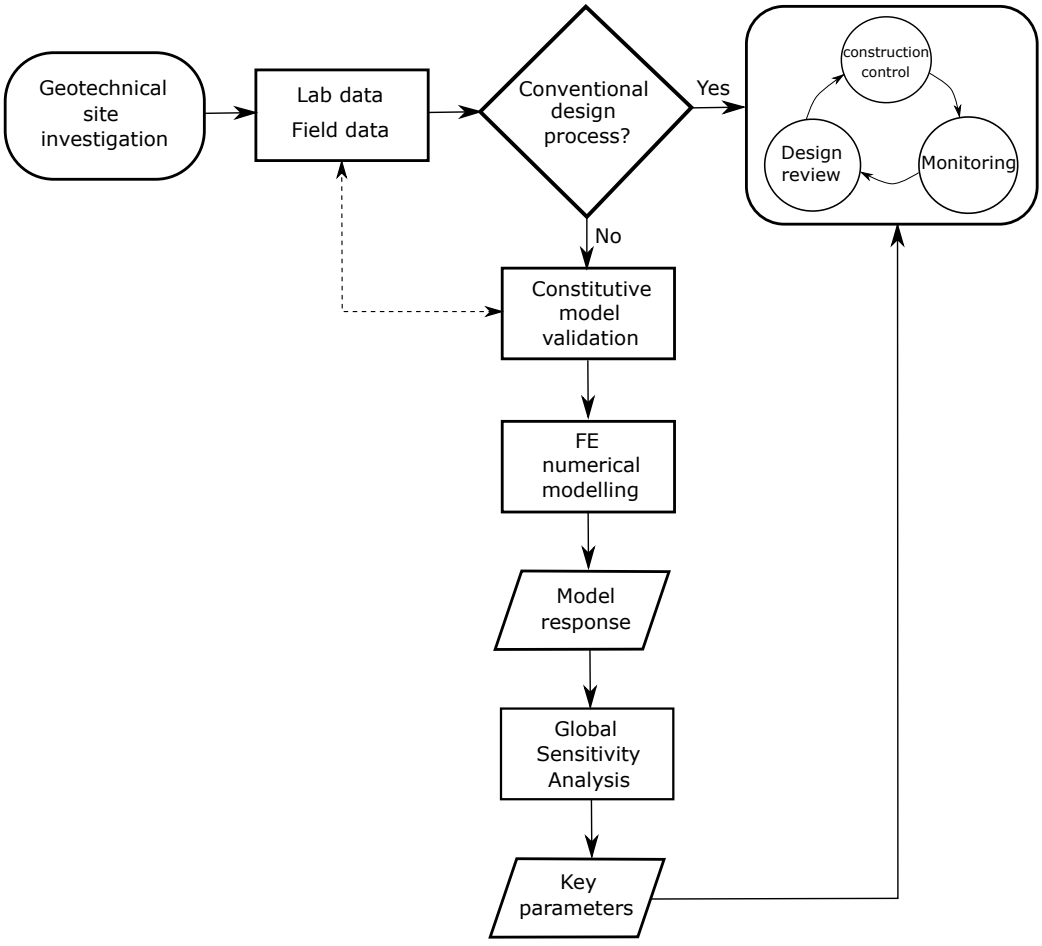

Figure 3.2: *The system for using GSA methods in FE modelling of geotechnical problems.*

FE simulations.

Furthermore, the temporal changes of sensitivity measures were revealed which is examined further in Paper B. Given the existence of several GSA methods, there was a necessity to identify the most suitable GSA approach for geotechnical FE modelling. By considering the complexity of existing advanced soft soil models and their high computational burden in numerical analyses, identifying the most feasible GSA method is an essential first step. Paper B discusses the process of assessing the Sobol method and factorial design in an FE model of Constant Rate of Strain (CRS). The problem has ample complexity, while at the same time being sufficiently simple in terms of geotechnical interpretation. Therefore, it is a suitable test case for benchmarking the two GSA methods considered. For the geotechnical models considered, the factorial design approach was proven to be more efficient in terms of computational time, required storage, and the amount of information obtained. Moreover, the sensitivity measures are corroborated spatially. The spatial comparison of sensitivities using two methods showed similar patterns.

Finally, the performance of Creep-SCLAY1Sc model for a Swedish clay has been investigated under cyclic loading with various amplitudes. As a result, a revised formulation for the strain accumulation of small loading amplitudes was developed. The newly proposed model is subsequently benchmarked against this new data set.

3.1 Global Sensitivity Analysis methods

A physical model is designed upon linear or non-linear relationships by relating the model parameters to the state variables of the system. Thus, model features are represented by their associated factors. Despite being involved in the system response, all factors are nonetheless not significant in a statistical sense. Sensitivity Analysis (SA) discovers the varying conditions of model behaviour due to uncertainty of input factors.

In general, SA is either performed locally or globally. The local SA examines the behaviour of the system due to variation of a single base point. A local SA around base point z_0 is obtained by taking the derivative of the system output Y over the input factor X_i. , *i.e.* Eq. (3.1).

$$\left| \frac{\partial Y}{\partial X_i} \right|_{z_0} \tag{3.1}$$

The local method does not predict accurate sensitivity measures when the model response is either nonlinear or uncertain. The global approach overcomes such limitations by exploring the effects of the entire factor space on the model response simultaneously. Therefore, the analyst is capable of capturing the possible interaction between model factors (Cacuci, 2003).

There are several techniques comprising Global Sensitivity Analysis: Elementary Effects (Morris, 1991), Variance-based methods, and Experimental design. Two major settings using GSA methods are sought (Saltelli, Ratto, et al., 2008):

(a) Factor prioritisation (FP): In this setting, the orders of the most influential factors causing variability in the model response is quantified.

(b) Factor fixing (FF): Fixing the inconsequential factors for subsequent model simplification in further analyses.

The typical features of the two GSA methods used in this study, namely the Sobol method and factorial design (FD), are explained briefly. Subsequently, the performance of the two methods is assessed in a geotechnical FE model presented in Paper B.

3.1.1 Sobol method

The Sobol method is a variance-based approach that takes into account output variance. It is a great advantage to use such a method because of its model independency, capability of measuring interaction effects, and incorporation of the entire range of factors for sensitivity analysis. The advantages mentioned, however, come with a high computational expense of estimating sensitivity indices, which is especially true for single runs with a significant amount of computational time.

Considering a deterministic analytical function f with k number of factors in which X_i is defined in a unit hypercube Ω^k:

$$
\begin{aligned}
&Y = f\left(X_i\right) \\
&\Omega^k = \left\{X_i | 0 \leq x_i \leq 1; \qquad \forall i = 1, \ldots, k\right\}
\end{aligned}
\tag{3.2}
$$

Sobol' (1993) decomposed function f into different dimensions:

$$
f = f_0 + \sum_{i=1}^{k} f_i + \sum_{i} \sum_{i<j} f_{ij} + \cdots + f_{12\ldots k} \tag{3.3}
$$

where in Eq. (3.3), f_0 is the average value of the function f:

$$
f_0 = \int_{\Omega^k} f(x) dx \tag{3.4}
$$

Sobol proves that the remaining terms of Eq. (3.3) are orthogonal in pairs. By assuming that f is square-integrable, the variance decomposition $V(Y)$ over the factor space Ω^k is derived (Sobol', 1993, 2001):

$$
V(Y) = \sum_{i=1}^{k} V_i + \sum_{i} \sum_{i<j} V_{ij} + \cdots + V_{12\ldots k} \tag{3.5}
$$

where in Eq. (3.5), $V_i = V(f_i)$ is the first-order variance of i^{th} parameter, and $V_{ij} = V(f_{ij})$ denotes the second-order variance contribution resulting from the interaction between factors i and j. The remaining higher-order interactions are considered up to $V_{1,\ldots,p}$, *i.e.* the interactions between all parameters.

The first-order index of Sobol is computed by normalising V_i over the total variance; see Eq. (3.6). A factor $\{X_i; \forall i = 1, \ldots, k\}$ is called important if it has a high value of S_i owing to a high V_i. In general, the first-order index shows the main contribution of each factor X_i on the variance of the model output $V(Y)$ (Saltelli, Tarantola, et al., 2000).

$$
S_i = \frac{V_i}{V} \tag{3.6}
$$

In linear (additive) models, the summation of first-order indices for all factors equals one (*i.e.* $\sum_{i=1}^{k} S_i = 1$). In non-linear models, these terms are less than one, *i.e.* $\sum_{i=1}^{k} S_i < 1$, due to the existence of interaction effects between parameters. This can be demonstrated by dividing Eq. (3.5) by $V(Y)$:

$$
\sum_{i=1}^{k} S_i + \sum_{i} \sum_{1 \leq i<j \leq p} S_{ij} + \sum_{i} \sum_{i<j} \sum_{i<j<m} S_{ijm} + \cdots + S_{12\ldots k} = 1 \tag{3.7}
$$

Eq. (3.7) shows that higher-order interaction effects play an important role as output variance for non-linear models. Therefore, Homma and Saltelli (1996) introduced a relatively economical approach for combining interactive effects and main effects. The total order index S_{T_i} is measured as Eq. (3.8), in which $V_{\sim i}$ denotes the resulting variance of Y taken over all factors except for the i^{th} factor.

$$S_{T_i} = 1 - \frac{V_{\sim i}}{V} \tag{3.8}$$

The total-order index quantifies the additivity of model parameters in the event of a significant difference between the first- and total-order indices. In general, S_{T_i} is used for factor fixing purposes, whereas S_i is mostly used for factor prioritisation (Saltelli, Ratto, et al., 2008).

3.1.1.1 Monte-Carlo sampling strategy for Sobol method

Saltelli (2002) employed quasi-random Monte-Carlo maps following the framework in Sobol' (1993) and the principle of parsimony. The sampling technique provides a remarkable reduction of computational costs, *i.e.* approximately half of the simulations generated from the traditional approach. The traditional sampling approach is more expensive but delivers more robust sensitivity measures (Saltelli, 2002). The numerical quasi-random Monte-Carlo approach consists of three initial steps in order to calculate sensitivity indices (Saltelli, Ratto, et al., 2008; Saltelli, Annoni, et al., 2010):

(i) Two random matrices $\boldsymbol{A}$ and $\boldsymbol{B}$ of dimension (N, k) are generated according to Eqs. (3.9) and (3.10).

$$\boldsymbol{A} = \begin{bmatrix} x_1^{(1)} & x_2^{(1)} & \dots & x_i^{(1)} & \dots & x_k^{(1)} \\ x_1^{(2)} & x_2^{(2)} & \dots & x_i^{(2)} & \dots & x_k^{(2)} \\ \vdots & \vdots & \ddots & \vdots & \ddots & \vdots \\ x_1^{(N-1)} & x_2^{(N-1)} & \dots & x_i^{(N-1)} & \dots & x_k^{(N-1)} \\ x_1^{(N)} & x_2^{(N)} & \dots & x_i^{(N)} & \dots & x_k^{(N)} \end{bmatrix}_{(N \times k)} \tag{3.9}$$

$$\boldsymbol{B} = \begin{bmatrix} x_{k+1}^{(1)} & x_{k+2}^{(1)} & \dots & x_{k+i}^{(1)} & \dots & x_{2k}^{(1)} \\ x_{k+1}^{(2)} & x_{k+2}^{(2)} & \dots & x_{k+i}^{(2)} & \dots & x_{2k}^{(2)} \\ \vdots & \vdots & \ddots & \vdots & \ddots & \vdots \\ x_{k+1}^{(N-1)} & x_{k+2}^{(N-1)} & \dots & x_{k+i}^{(N-1)} & \dots & x_{2k}^{(N-1)} \\ x_{k+1}^{(N)} & x_{k+2}^{(N)} & \dots & x_{k+i}^{(N)} & \dots & x_{2k}^{(N)} \end{bmatrix}_{(N \times k)} \tag{3.10}$$

(ii) Create matrix $\boldsymbol{C}_i$ by using a copy of $\boldsymbol{B}$ but replacing the ith column from $\boldsymbol{A}$.

$$\boldsymbol{C}_i = \begin{bmatrix} x_{k+1}^{(1)} & x_{k+2}^{(1)} & \dots & x_i^{(1)} & \dots & x_{2k}^{(1)} \\ x_{k+1}^{(2)} & x_{k+2}^{(2)} & \dots & x_i^{(2)} & \dots & x_{2k}^{(2)} \\ \vdots & \vdots & \ddots & \vdots & \ddots & \vdots \\ x_{k+1}^{(N-1)} & x_{k+2}^{(N-1)} & \dots & x_i^{(N-1)} & \dots & x_{2k}^{(N-1)} \\ x_{k+1}^{(N)} & x_{k+2}^{(N)} & \dots & x_i^{(N)} & \dots & x_{2k}^{(N)} \end{bmatrix}_{(N \times k)} \tag{3.11}$$

(iii) The model outputs of dimension $(N \times 1)$ are calculated using the samples generated by

matrices $\boldsymbol{A}$, $\boldsymbol{B}$, and $\boldsymbol{C}_i$.

$$\begin{aligned} \boldsymbol{y}_{A_{(N\times 1)}} &= f(\boldsymbol{A}) \\ \boldsymbol{y}_{B_{(N\times 1)}} &= f(\boldsymbol{B}) \\ \boldsymbol{y}_{C_{i(N\times 1)}} &= f(\boldsymbol{C}_i) \end{aligned} \tag{3.12}$$

By recalling Eqs. (3.6) and (3.8) and following the Monte-Carlo procedure above, the first-order and total-order indices are calculated as Eqs. (3.13) and (3.14):

$$S_i = \frac{V_i}{V} = \frac{\boldsymbol{y}_A^{\intercal} \cdot \boldsymbol{y}_{C_i} - f_0^2}{\boldsymbol{y}_A^{\intercal} \cdot \boldsymbol{y}_A - f_0^2} \tag{3.13}$$

$$S_{T_i} = 1 - \frac{V_{\sim i}}{V} = 1 - \frac{\boldsymbol{y}_B^{\intercal} \cdot \boldsymbol{y}_{C_i} - f_0^2}{\boldsymbol{y}_A^{\intercal} \cdot \boldsymbol{y}_A - f_0^2} \tag{3.14}$$

where f_0 is defined as Eq. (3.15) conforming to Eq. (3.4):

$$f_0 = \frac{1}{N} \sum_{j=1}^{N} y_A^{(j)} \tag{3.15}$$

3.1.2 Factorial design

Regardless of the local and global classifications, a common sensitivity approach performed by scientists and engineers is a series of One-Factor-At-a-Time (OFAT) experiments. In that approach, the model response is evaluated by changing one factor while keeping others constant. Several authors have highlighted the inefficiency and disadvantages of the OFAT approach compared to the designed experiments (*e.g.* Daniel, 1973; Czitrom, 1999; Saltelli and Annoni, 2010).

Fisher (1942) introduced factorial design in experimentation, *i.e.* a statistically designed approach that varies certain factors to study experimental responses simultaneously. The factors of interest are determined primarily and different levels are associated with each factor. In a full factorial scheme, all potential combinations of factors are used. The main advantage of a full design lies in providing adequate information upon the series of responses associated with each trial, denoted as the main effects of factors. Additionally, the effects of a single variable may originate in the variation of other factors, *i.e.* an interaction effect. Factorial design quantifies possible interaction effects towards a specific model response (Daniel, 1976; Box, Hunter, et al., 2009).

As an example, a full factorial design considering two factors A and B are shown in Table 3.1. Two levels corresponding to the lower and upper bounds are associated with each factor, respectively. Following the factorial sampling scheme, a table including all possible combinations of the $-$ and $+$ levels can be created as shown in Table 3.2. This is denoted a *table of contrast* and consists of a set-up of parameters (columns A and B) corresponding to each realisation (*i.e.* Run #). Additionally, the AB column that captures interaction between the two parameters is added. The chosen response of each realisation is shown as a single observation, *i.e.* denoted by y.

Table 3.1: Levels of factors: a 2^2 example.

	Levels	
Factors	−	+
A	A^-	A^+
B	B^-	B^+

Table 3.2: Table of contrast for the 2^2 full factorial design.

Run #	A	B	AB	Response, y
1	−	−	+	y_1
2	+	−	−	y_2
3	−	+	−	y_3
4	+	+	+	y_4

Considering the two-level factorial design, the main and interaction effects are obtained using Eq. (3.16). $\mathbf{C}_m$ is denoted as a contrast matrix, $\mathbf{R}$ as a response vector, $\mathbf{E}$ as a vector of effects, and n_{runs} the total number of runs in a two-level factorial design. Furthermore, $A_{\text{main.}}$ and $B_{\text{main.}}$ are the calculated main effects of factors A and B. Finally, $AB_{\text{int.}}$ measures the interaction effect between factors A and B.

$$\mathbf{E} = \frac{2}{n_{\text{runs}}} \underbrace{\begin{bmatrix} -1 & -1 & +1 \\ +1 & -1 & -1 \\ -1 & +1 & -1 \\ +1 & +1 & +1 \end{bmatrix}^{\mathsf{T}}}_{\mathbf{C}_m^{\mathsf{T}}} \underbrace{\begin{bmatrix} y_1 \\ y_2 \\ y_3 \\ y_4 \end{bmatrix}}_{\mathbf{R}} = \begin{bmatrix} A_{\text{main.}} \\ B_{\text{main.}} \\ AB_{\text{int.}} \end{bmatrix} \tag{3.16}$$

3.1.2.1 Fractional factorial design

Through an initial exploration of a process, a screening approach is often performed to determine a small number of factors that have significant effects on a response. This is achieved by fractionation of a full factorial, hence leading to interactive effects that confound main effects. The amount of confounding in a fractional design is introduced by the term *resolution*. In a design of *resolution IV*, the main effects are not confounded by two-factor interactions; however, one two-factor interaction is confounded by another two-factor interaction.

The main concept of the fractional factorial approach lies in confounding specific interactions by main effects; thus, the total number of experiments decreases dramatically. As a result, it is not possible to measure the interactions between parameters. Therefore, it is often used as a first step for screening experiments prior to full factorial design. Designing a fractional factorial comes with choosing a *resolution* that governs the degree of confounding (see *e.g.* Box, Hunter, et al., 2009; Montgomery, 2009).

3.1.3 Cyclic accumulation model

Full details of the following model development and performance are discussed in Paper C.

3.1.3.1 The concept of strain resistance

Janbu (1969) introduced the resistance concept for deformation of soils. The resistance of a medium, or any control volume thereof, is defined as:

$$R = \frac{\text{differential cause}}{\text{differential effect}} \tag{3.17}$$

Later on, Janbu (1976) suggested that the resistance concept is also applicable to effective stress interpretation of cyclic loads. For a given soil under cyclic loading with a constant amplitude (deviatoric stress), the tangent to the cause-effect curve is equal to the resistance; see Fig. 3.3. Hence, the strain resistance R_ϵ is written as Eq. (3.18), in which N is the number of cycles, and ϵ is the accumulated strain.

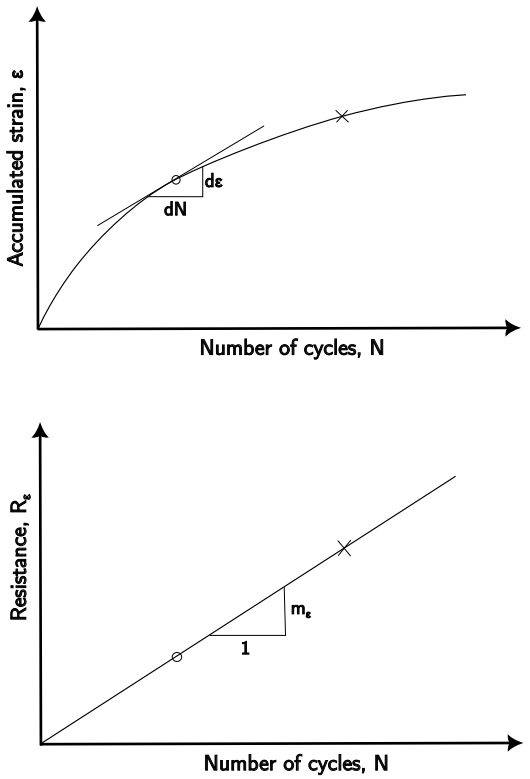

Figure 3.3: *Determination of cyclic strain resistance (Janbu, 1976).*

$$R_\epsilon = \frac{dN}{d\epsilon} \tag{3.18}$$

For most experimental data on overconsolidated clays (including naturally sensitive clays in Sweden that are slightly overconsolidated due to creep processes), the R_ϵ increases almost linearly with the number of cycles N, as sketched in the lower part of Fig. 3.3 (Janbu, 1976). Thus, Eq. (3.19) is expressed as follows:

$$R_\epsilon = m_\epsilon N \tag{3.19}$$

In Eq. (3.19), m_ϵ is a dimensionless resistance number for strain accumulation. The change in (viscoplastic) volumetric strain is derived as Eq. (3.20).

$$\Delta\epsilon_v^{vp} = \frac{1}{m_\epsilon} \ln N \tag{3.20}$$

Furthermore, the isotropic part of the hardening rule in the base model used, Creep-SCLAY1S, is given in Eq. (3.21) (Gras et al., 2018):

$$\frac{dp'_p}{d\epsilon_v^{vp}} = \frac{p'_p}{\zeta_i^*} \qquad \text{where} \quad \zeta_i^* = \lambda_i^* - \kappa^* \tag{3.21}$$

in which, ζ_i^* is an intrinsic parameter related to the irrecoverable compression, κ^* is the modified swelling index, and λ_i^* is the modified intrinsic compression index. Integration of Eq. (3.21), over equivalent mean effective stress p'_{eq} to the projected stress that corresponds to the size of NCS p'_p, results in:

$$\Delta\epsilon_v^{vp} = \zeta_i^* \ln\left(\frac{p'_p}{p'_{eq}}\right) \tag{3.22}$$

Equating Eqs. (3.18) and (3.19) provides:

$$\frac{dN}{d\epsilon} = m_\epsilon N \tag{3.23}$$

By combining Eqs. (3.20), (3.22) and (3.23), and introducing time by $t = NT$, in which T is the loading period for cyclic loading, yields:

$$\frac{d\epsilon_v^{vp}}{dt} = \frac{1}{m_\epsilon T}\left(\frac{p'_{eq}}{p'_p}\right)^{m_\epsilon \zeta_i^*} \tag{3.24}$$

3.1.3.2 Revised formulation for cyclic accumulation

The proposed constitutive model follows a similar strain decomposition as the original Creep-SCLAY1S model, except for the inclusion of a cyclic component in the viscoplastic strain tensor which follows the Creep-SCLAY1Sc model:

$$\dot{\epsilon} = \dot{\epsilon}^e + \underbrace{(\dot{\epsilon}^c + \dot{\epsilon}^{cyc})}_{\dot{\epsilon}^{vp}} \tag{3.25}$$

where in Eq. (3.25), $\dot{\epsilon}^e$ is the tensor of elastic strain rate, $\dot{\epsilon}^{vp}$ viscoplastic strain rate, $\dot{\epsilon}^c$ the creep strain rate, and $\dot{\epsilon}^{cyc}$ cyclic strain rate. An additional viscoplastic multiplier $\dot{\Gamma}$ that captures the cyclic accumulation is added to the original creep viscoplastic multiplier; thus, $\dot{\epsilon}^{vp}$ becomes:

$$\dot{\epsilon}^{vp} = \left[\dot{\Lambda} + \dot{\Gamma}\right] \frac{\partial p'_{eq}}{\partial \boldsymbol{\sigma}'} \tag{3.26}$$

Equation (3.26) implies that the viscoplastic strain resulting from the cyclic loading follows the same direction as the viscoplastic creep strain; therefore, the associated flow rule is maintained. Referring to Eq. (3.24) and by introducing ψ which scales the impact of the 'overconsolidation ratio' on the magnitude of cyclic accumulated strain, the viscoplastic multiplier for cyclic accumulation is defined as:

$$\dot{\Gamma} = \frac{1}{|m_\epsilon| T} \left(\frac{p'_{eq}}{p'_p}\right)^{\psi \zeta_i^*} \tag{3.27}$$

The creep viscoplastic multiplier in Eq. (2.5), in terms of Janbu's resistance concept, can be rewritten as Eq. (3.28). In the following, r_{si} is denoted as the intrinsic time resistance number (Grimstad et al., 2010).

$$\dot{\Lambda} = \frac{1}{r_{si}\tau} \left(\frac{p'_{eq}}{p'_p}\right)^{r_{si}\zeta_i^*} \left(\frac{M(\theta)^2 - \alpha^2_{K_0^{nc}}}{M(\theta)^2 - \eta^2_{K_0^{nc}}}\right) \tag{3.28}$$

3.1.4 Small-strain stiffness formulation

The small-strain stiffness formulation is implemented as part of the calculation of the elastic stiffness matrix D_{ijhk}. A 6×6 stiffness matrix following Hooke's law, where the elastic stiffness in the overconsolidated region κ^*, the Poisson ratio ν from Creep-SCLAY1S is used with the mean effective stress p' to first calculate the shear modulus G as Eq. (3.29):

$$G = \frac{3p'(1-2\nu)}{2\kappa^*(1+\nu)} \tag{3.29}$$

the values of D_{ijhk} are determined as shown in equation Eq. (3.30), where the Kronecker delta is denoted using the index notation of δ.

$$D_{ijhk} = \frac{2G\nu}{1-2\nu}\delta_{ij}\delta_{hk} + G(\delta_{ik}\delta_{jh} + \delta_{ih}\delta_{jk}) \tag{3.30}$$

The small-strain extension, proposed herein, replaces G with an expression that depends on the strain history, and the highest attainable stiffness at small strain G_{max}. There are many options (*e.g.* Hardin and Drnevich, 1972; Darendeli, 2001), however, in this thesis a suggestion by Sivasithamparam, D'Ignazio, et al. (2021) is followed, *i.e.*:

$$G = G_{max}\left[1 - \frac{\langle \varepsilon_q - \varepsilon_s \rangle}{A + B\langle \varepsilon_q - \varepsilon_s \rangle}\right] \tag{3.31}$$

where G_{max} is the reference stiffness at small strain and will be reduced towards a limiting value that is controlled by parameters A and B and the shear strain history. The initial reference stiffness at small strain is derived by inserting Eq. (3.32) into Eq. (3.29). The deviatoric component of the total shear strain ε_q is compared to a threshold value ε_s, which is an internal variable fixed at 10^{-5}. The symbols $\langle \bullet \rangle$ are Macaulay brackets that return $(\varepsilon_q - \varepsilon_s)$ for $(\varepsilon_q - \varepsilon_s) > 0$ and 0 otherwise.

$$\kappa_0^* = \frac{\kappa^*}{\varpi} \tag{3.32}$$

A and B are chosen such that G ranges between G_{max} and G at engineering strain levels. By rearranging Eq. (3.31), the true limit when $\langle \varepsilon_q - \varepsilon_s \rangle \to \infty$ is:

$$\lim_{\langle \varepsilon_q - \varepsilon_s \rangle \to \infty} \left[1 - \frac{\langle \varepsilon_q - \varepsilon_s \rangle}{A + B \langle \varepsilon_q - \varepsilon_s \rangle} \right] = 1 - \frac{1}{B} \tag{3.33}$$

Thus, the model parameter B is related to the unload/reload shear modulus (the stiffness in the overconsolidated regime) G_{ur} as a transition towards the larger strains, see Eq. (3.34).

$$B = \frac{1}{1 - \frac{G_{\text{ur}}}{G_{\text{max}}}} \tag{3.34}$$

4 Experimental data

As part of the project, laboratory tests were conducted to study the cyclic degradation response of a Swedish clay (Dijkstra et al., 2022), and some of the results and the text in the following are further detailed in Paper C.

The tests were performed on intact samples of Swedish clay collected from the Kärra test site in northern Gothenburg. The samples were extracted from a depth of 9 m using a Swedish STII sampler (SGF, 2009). The clay is classified as CH (fat clays) under the unified Soil Classification System and is positioned above the A-line in the Casagrande plasticity chart. The properties displayed in Table 4.1 were obtained from the classification tests.

Table 4.1: Index properties of Kärra clay. ρ_b bulk density; w_N natural water content; S_t sensitivity (fall cone).

Depth	ρ_b	Liquid Limit	Plastic Limit	Plastic Index	w_N	S_t
m	g m^{-3}	%	%	%	%	-
9	1.58	75.2	27.6	47.6	71.6	6.4

As shown in Fig. 4.1 the composition of the clay was determined to be 71 % clay with illite as the main clay mineral, 28 % silt. The groundwater table at the site is located near the surface, leading to an *in-situ* stress state with a mean effective stress p'_0 of 52 kPa and a deviatoric stress q_0 of 28 kPa. The average shear modulus, which was determined at comparable depths and similar geological deposition in nearby sites with a seismic dilatometer, was found to be $G_{max} = 17.5 \pm 2.5$ MPa (Wood, 2016).

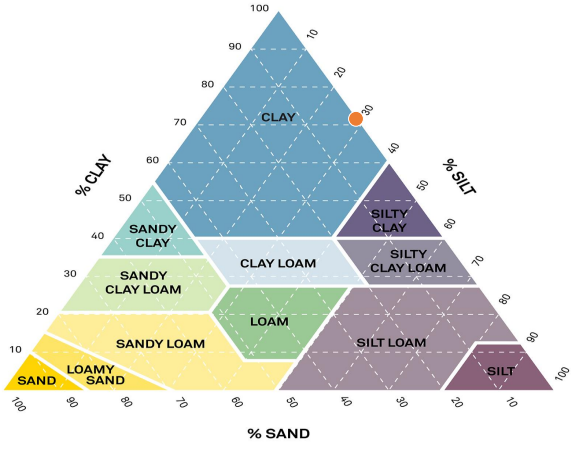

Figure 4.1: *Composition of Kärra clay from* 9 m *depth.*

4.1 Test setup

A computer-controlled hydraulic stress path apparatus of Bishop and Wesley (1975) was modified for performing cyclic loading tests on 50 mm diameter and 100 mm tall specimens. To measure the axial strains, external Linear Variable Differential Transducers (LVDTs) were utilised in all experiments. Due to the low stiffness of the samples tested, the use of external LVDT was considered sufficient for accurate measurements, as confirmed through a comparison to tests that had additional local instrumentation of two submersible LVDTs attached to the middle section of the sample (Dijkstra et al., 2022). As a result, all experimental data used in this thesis are considered to have a similar level of accuracy.

The porewater pressures were measured at the bottom of the specimen. To accurately track the changes in porewater pressures during undrained cyclic loading, the cyclic load was applied at a slow rate (a sinusoidal load with period of $T = 180$ s). A suction cap was used in order to perform cyclic loading in the extension regime and to balance the load between the load cell and top plate. Paper side drains were utilised to speed up the consolidation stage. Paraffin oil was used for the fluid in the triaxial cell, whereas the back pressure lines were filled with tap water. During the consolidation, undrained pre-shearing and cyclic loading stages, Global Digital Systems (GDS) controllers were used to regulate cell, back, and ram pressures with a precision exceeding 0.5 kPa.

4.2 Experimental procedure

Eight undrained cyclic triaxial tests were performed on high-quality cylindrical undisturbed samples extracted from 9 m depth. After assessing the monotonic results of the undrained anisotropically consolidated compression (CAUC) tests, only samples from 9 m depth were used for the cyclic tests. The systematic testing of samples from a single depth enables isolating the impact of pre-shearing and loading amplitude; thus, simplifies the calibration procedure. As such, the complete test was stress controlled, whereas the emerging (accumulated) strains and (excess) porewater pressures were measured during the test. The stages of the tests, along with their specifications, are presented in Table 4.2.

The testing procedure consisted of multiple stages, which are outlined as follows:

1. The specimens were subjected to an anisotropic consolidation stage through the application of the deviatoric stress q_0, which was representative of the *in-situ* conditions. An average of one day was required to complete the anisotropic consolidation of the sample, as indicated in Table 4.2.

2. A stage dedicated to equalising the porewater pressures was conducted after the consolidation stage had been completed.

3. An undrained pre-shearing stage, with the extent of q_p, was incorporated in some of the tests, such as Test 04, Test 08, Test 10, and Test 11. These tests included a subsequent creep stage following loading/unloading as detailed in Table 4.2.

4. In the undrained cyclic loading stage, the superimposed deviatoric stress q_m was subjected to an undrained cyclic loading with amplitude q_{cyc}. To ensure that the maximum stress level remained below the critical limit, q_{cyc} was selected such that the combined deviatoric

stress, $q_m + q_{\text{cyc}}$, was less than twice the undrained shear strength, represented by $q_{\max}$. The undrained shear strength was determined through monotonic CAUC test, resulting in a value of $s_u = 33\,\text{kPa}$.

The purpose of the laboratory tests was to understand the impact of pre-loading, such as from embankment construction or excavation, on the soil response to cyclic loading. Two data series were designed to accomplish this objective. In the first series, the superimposed deviatoric stress q_m was kept constant while the cyclic loading amplitude q_{cyc} was varied. In the second series, the samples underwent an undrained pre-shearing stage, which resulted in a variation of q_m while keeping q_{cyc} constant.

Tests 05, 06, 07, and 09 were anisotropically consolidated and subjected to a first creep stage prior to cyclic loading. In contrast, Tests 04, 08, 10 and 11 included a pre-shearing stage followed by a second creep stage before cyclic loading. The long duration of creep stages, lasting for several days, provided the opportunity to distinguish the deviatoric creep under a constant load from the impact of cyclic loading. This also contributed to the slight variation in the values of p'_0 and q_0 obtained after the consolidation stage, as presented in Table 4.2. The creep stages were also performed to balance the porewater pressures after both the consolidation and pre-shearing stages.

Following the completion of the experiments, some fluctuations were noted in the axial strain readings, particularly in Test 10 and the latter part of Test 07. The data from tests that include pre-shearing, with the exception of Test 10, will be employed to verify the accuracy of the constitutive model when dealing with loading scenarios that are more intricate. Meanwhile, the data obtained from the first series of tests will be employed to refine the hardening law in the model.

5 Summary of Appended Papers

The process and main findings are briefly summarised below.

Paper A: "Towards rigorous boundary value level sensitivity analyses using FEM"

The GSA methodology is implemented for the purpose of evaluating the example of coupled hydro-mechanical response of Creep-SCLAY1S in oedometric conditions. In particular, the linkage of the Sobol method to the numerical Finite Element framework was assembled using Tochnog Professional and SALib (Herman and Usher, 2017). As such, the incremental loading oedometer test is modelled at the boundary value level, where an increment in load leads to the generation and subsequent dissipation of excess porewater pressures. The SA results indicate that the priority of certain model parameters is dependent on the magnitude of the load step relative to the apparent pre-consolidation pressure. Concerning the model investigated, κ^* governed the initial response of the compression curve, the OCR dominated the step close to pre-consolidation pressure, and λ_i^* was the most significant parameter representing the largest stress levels. The Sobol results from three different load steps in coupled analyses at a boundary value level of the 1D incremental loading oedometer test is shown in Fig. 5.1.

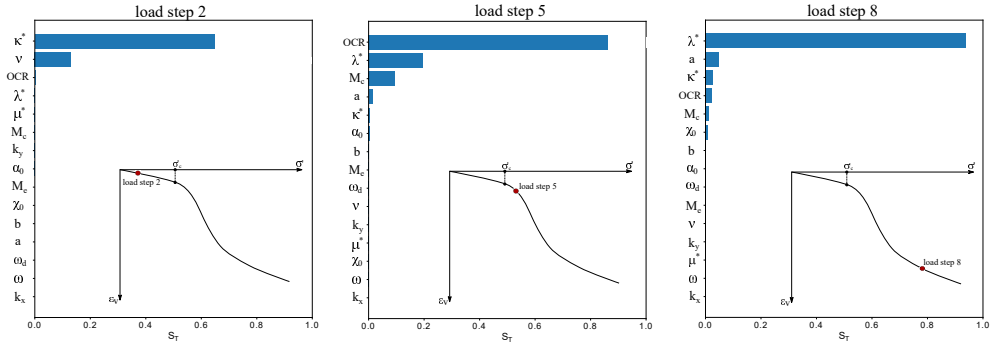

Figure 5.1: *Creep-SCLAY1S sensitivity analysis using Sobol method. The total-order index of three load steps are presented.*

Paper B: "Using experimental design to assess rate-dependent numerical models"

The Experimental Design was benchmarked against the Sobol method. The assessment was performed using Creep-SCLAY1S in a numerical analysis of a well-defined case; a constant rate of strain (CRS) test. Based on the different response of the (slightly) overconsolidated clays over time, the effective stress-strain behaviour of the CRS simulation is separated into three Zones shown in Fig. 5.2.

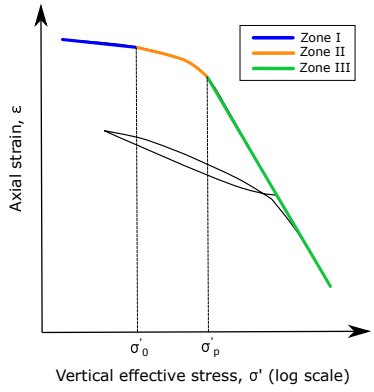

Figure 5.2: *Definition of zones in effective stress-strain consolidation curve of an overconsolidated sample (Adapted from Peck et al., 1974).*

Following a temporal Sensitivity Analysis (SA), the parameters that exhibit a significant impact were determined to be the *active* parameters for each designated Zone; see Eq. (5.1). The parameters underlined in Eq. (5.1) were found to be the most influential parameters for calibrating the CRS boundary value problem through the utilisation of Creep-SCLAY1S.

$$\text{Zone I} = \left\{\underline{\kappa^*}, \underline{u}, \nu', \alpha_0\right\} \tag{5.1a}$$

$$\text{Zone II} = \left\{\underline{\sigma'_{p_0}}, \underline{M_c}, \underline{\lambda_i^*}, \underline{a}, \kappa^*, u\right\} \tag{5.1b}$$

$$\text{Zone III} = \left\{\underline{\lambda_i^*}, \underline{a}, \underline{\chi_0}, u, b, \sigma_{p_0}, M_c, \alpha_0\right\} \tag{5.1c}$$

By investigating the temporal sensitivities in detail, it was acknowledged that the ranking of the important parameters evolves over time. The methodology presented in Paper B systematically identifies the active parameters that result in unique solutions. Fig. 5.3(a) demonstrates the issue of non-uniqueness that arises from variation of parameter ω, while other parameters are held constant. This results in similar stress-strain behaviour being obtained by merely altering the non-influential parameter ω. In contrast, Fig. 5.3(b) showcases that the governing parameters determined through the temporal SA, such as λ_i^*, results in unique solutions within their respective influential Zones.

The spatial sensitivity measures based on both GSA methods are not that distinct, meaning that Experimental Design is also capable of distinguishing spatial sensitivity as the Sobol method;

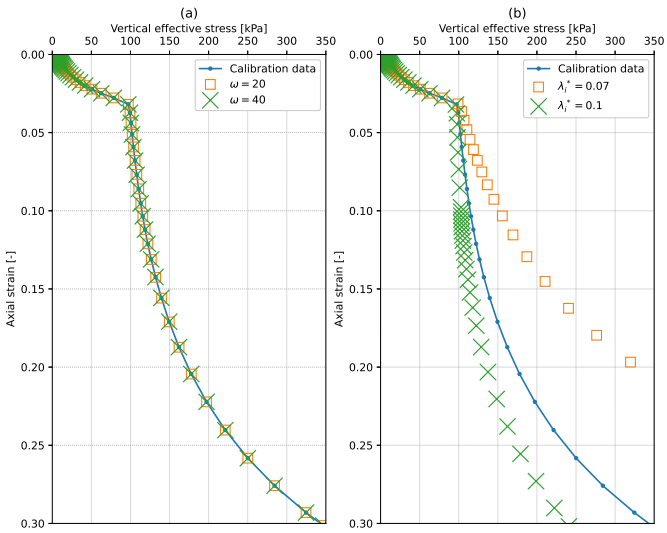

Figure 5.3: *Non-uniqueness of parameter sets in CRS loading path using Creep-SCLAY1S. (a) Non-uniqueness observed for parameter ω. (b) Unique curves obtained after changing parameter λ_i^*, shown after preconsolidation pressure.*

see Fig. 5.4. Furthermore, the spatial figures demonstrate different sensitivity measures in very different areas of the numerical model. For example, the impact of the displacement rate was most pronounced near the top boundary for both techniques. Thus, the application of GSA methods for numerical modelling of geotechnical problems opens up a rigorous design for monitoring schemes, as the importance of factors towards a model outcome can be quantified in numerical mesh.

Paper C: "Low amplitude strain accumulation model for natural soft clays below railways"

In this paper, a low amplitude cyclic accumulation model was developed, after establishing that Creep-SCLAY1Sc was not adequately capturing low-amplitude results from a new series of undrained cyclic triaxial tests on anisotropically consolidated Kärra clay. The cyclic accumulation formulation was based on Janbu's resistance concept and employed as part of the Creep-SCLAY1Sc model. Furthermore, a small-strain stiffness formulation was implemented.

The response of the undrained cyclic triaxial experiments have been analysed. Based on the current experiments, a critical stress threshold was identified for cyclic failure of the test specimens. Experiments with pre-shearing stages exhibit lower resistance number m_ϵ than those without pre-shearing, as depicted in Fig. 5.5. In addition, an exponential relation was approximated between the resistance number and stress ratio q_{cyc}/p'_0 .

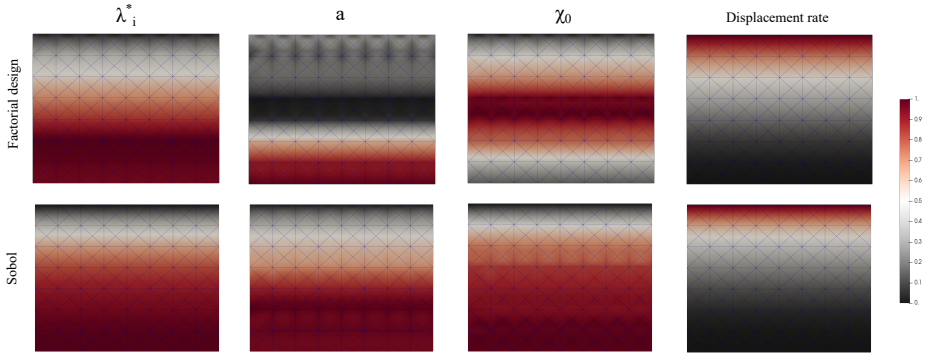

Figure 5.4: *Comparison of sensitivity measures for two Global Sensitivity Analysis (GSA) methods. The Sobol and Experimental design were used to perform the SA with respect to σ'_{yy} at 30 % vertical strain.*

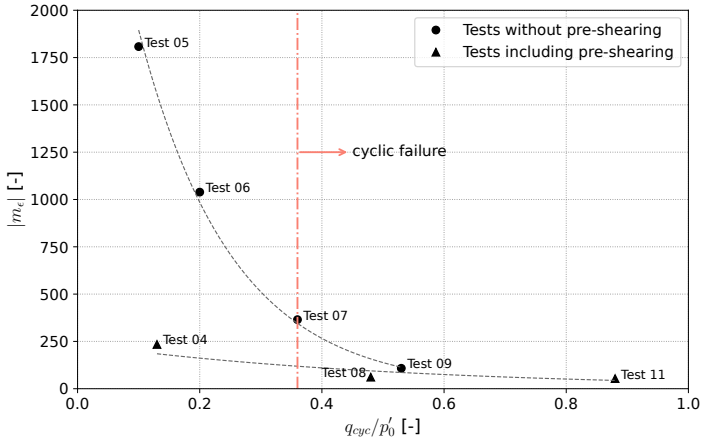

Figure 5.5: *Relationship between the degree of shear mobilisation (q_{cyc}/p'_0) and the resistance number (m_ϵ) for Kärra samples obtained from undrained cyclic triaxial tests.*

Simulations were carried out on both low- and high-amplitude tests performed on Kärra tests specimens. Fig. 5.6 shows the results from Test 09, *i.e.* a test with high loading amplitude. A good agreement between simulation and experimental behaviour was observed for the measured axial strain. However, the excess porewater pressure was overestimated by a sudden jump in the initial phase of the simulation which probably was due to the stiffness response of the model, although further investigations will address this issue. Fig. 5.7 demonstrates the behaviour of the model versus a test with relatively low loading amplitude. It is concluded that the model is able to capture the behaviour of the clay under low loading amplitudes, *i.e.* crucial for SLS modelling of railway embankments over a long period of time.

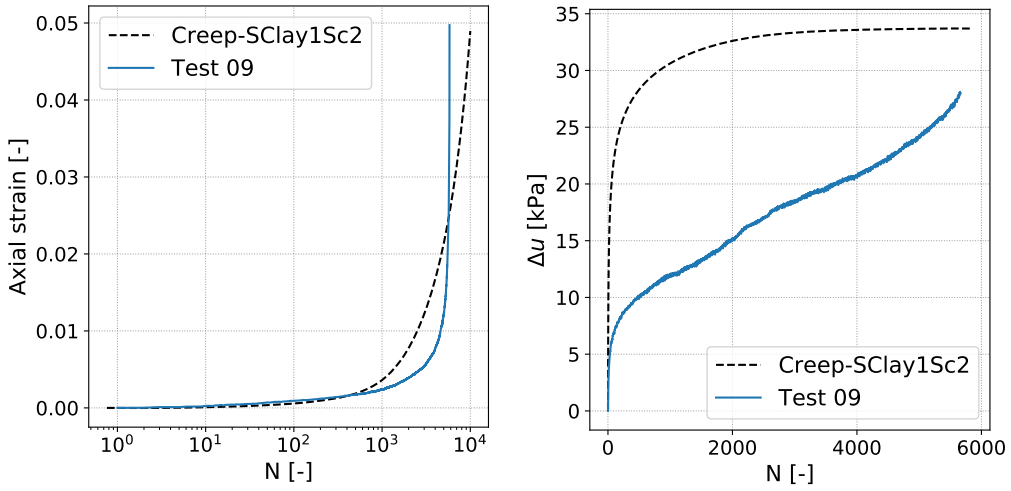

(a) (b)

Figure 5.6: *Example of a high amplitude test with* $q_{cyc} = 28\,\text{kPa}$

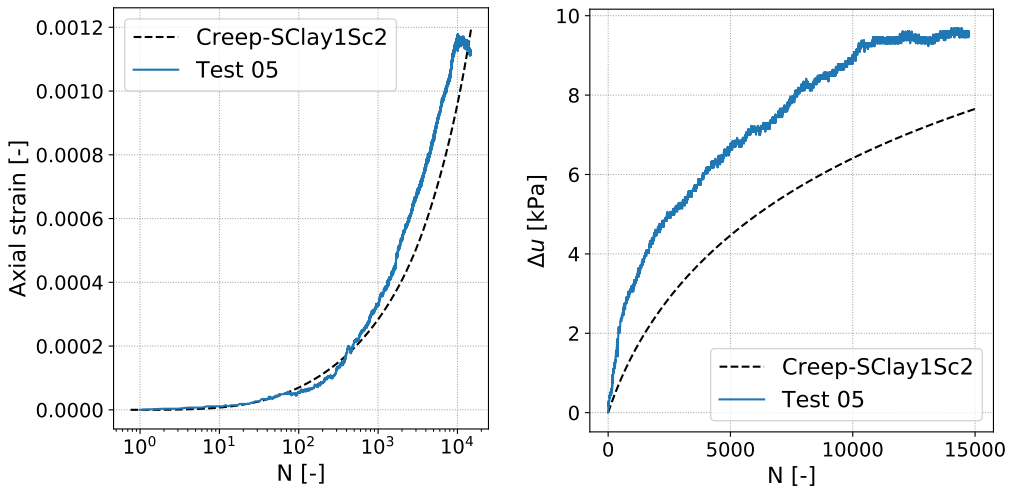

(a) (b)

Figure 5.7: *Example of a low amplitude test with* $q_{cyc} = 5\,\text{kPa}$

6 Conclusions and outlook

This thesis is divided into two parts. The aim of the first part has been to implement Global Sensitivity Analysis (GSA) methods for geotechnical problems using Finite Element (FE) analysis. The study focused on advanced constitutive models developed for soft natural clays, incorporating rate-dependency, anisotropy, and bond degradation. The models in the first part included the viscoplastic Creep-SCLAY1S model. In the second part, a revised cyclic model for low loading amplitudes was developed (Paper C).

Two GSA methods, *i.e.* Experimental design and Sobol method, were successfully implemented for evaluating the behaviour of Creep-SCLAY1S in a boundary value problem. The application of GSA methods to geotechnical Finite Element Analyses (FEA) enables a rigorous assessment of the model output, both along temporal and spatial scales. By analysing the significant geotechnical parameters of the model response in time and space, the costs associated with using advanced models that require a comprehensive site investigation are potentially reduced. Furthermore, GSA opens up the rigorous design of monitoring schemes, as the importance of model parameters towards a model outcome (*e.g.* settlements or horizontal displacements at the toe of an embankment) can be quantified.

The main conclusion of the first part is that the Sobol method is overly computationally expensive for geotechnical FEA due to its Monte-Carlo sampling strategy. It was shown that Experimental design was a viable alternative to the Sobol method at a boundary value level (Paper B). The spatial sensitivity analysis using the two GSA methods demonstrated similar patterns linked to the evolution of effective stress. The temporal analyses of the sensitivity measures using Experimental design have illustrated factor prioritisation changes at different stages of the CRS test. Therefore, the entire time domain spectrum should be investigated for factor fixing of rate-dependent problems. The methodology proposed in this study has high potential for assessing comprehensive models (*e.g.* Creep-SCLAY1S) that capture complex soil features. Therefore, the methodology can be employed as an essential step prior to inverse modelling, data assimilation, and Random Finite Element Method (RFEM). There is also an opportunity to conduct optimal experimental design to enhance the reliability of predictions based on model updating and data monitoring in real scale infrastructure projects.

In the second part of the study, the cyclic response of a soft natural clay from Sweden has been studied by means of a series of undrained cyclic triaxial tests at different loading amplitudes. The testing of smaller load amplitudes, which are more commonly observed in soft soils below railway infrastructure, distinguishes the current thesis from previous studies such as that of Zuada Coelho et al. (2021). Some tests included a pre-shearing stage to isolate the impact of loading amplitude from the effect of pre-loading, such as embankment construction or an excavation. It appears that below a critical stress ratio (*i.e.* $q_{\mathrm{cyc}}/p'_0 <\approx 0.35$ in this study), failure was not reached due to undrained cyclic loading. This is in line with prior findings where the mean effective stress level is an important factor for cyclic failure of clays. Furthermore, undrained pre-shearing prior to cyclic loading had a considerable effect on the magnitude of cyclic resistance, as samples with pre-shearing exhibited a lower resistance number. In addition, the relationship between the cyclic resistance and number of cycles was found to be almost linear, supporting the findings of Janbu (1976). An exponential relation between the resistance number and degree of shear mobilisation was established.

The cyclic behaviour of the clay tested at lower loading amplitudes is primarily manifested as a creep phenomenon, exhibiting higher creep rates than those resulting from deviatoric creep alone. However, the accuracy of the Creep-SCLAY1Sc model, which was developed for large amplitudes, when calibrated with a new data set, was found to be lacking at stress ratios below the critical value. Consequently, a revised strain accumulation model that incorporates Janbu's resistance concept and an additional feature for small-strain stiffness was derived to simulate the cyclic loading of soft natural clays at low stress amplitudes.

The revised strain accumulation model, which retains the advanced features of Creep-SCLAY1S, incorporates a modified viscoplastic multiplier and a strain dependent stiffness formulation for a smooth transition between the stiffness at small strain and engineering levels. Based on the calibration carried out using the data set presented in this thesis, the predictions of the revised model proved to be accurate for both low and high amplitude tests, as well as independent tests that underwent pre-shearing. Ultimately, this model serves as a basis for modelling the strain accumulation under railway embankments constructed on soft natural clays over a large number of loading cycles. However, further investigation is required to evaluate the stable phases of low amplitude tests at high cycle numbers, where strain accumulation reaches stability.

Given the limited information available on the degradation of railway foundations, especially with regard to the foundation, conducting field experiments to observe degradation effects under natural conditions is crucial. Besides, more laboratory data on the cyclic response of Swedish natural clays at different stress-ratios and with different loading periods are required to broaden the understanding of resistance numbers for natural clays. Additional data could lead to the improvement of predictive models and enhance the ability to estimate the lifespan of railway structures with greater precision. The current test programme and test stage design for the experimental campaign incorporated long duration creep stages, resulting in a change of state in the sample, which needs to be incorporated in the numerical analyses. Some of the experimental choices, however, complicated the model development process. A future test test programme should adopt the best practices of Experimental design to overcome this limitation. Finally, when developing rate-dependent models, all aspects of the experiment that are time-dependent (consolidation, pore-water pressure equalisation, creep, cyclic strain accumulation) should be considered during the model development process and accounted when performing model simulations.

References

Alves Costa, P., Calçada, R., Silva Cardoso, A., and Bodare, A. (2010). "Influence of soil non-linearity on the dynamic response of high-speed railway tracks". In: *Soil Dynamics and Earthquake Engineering* 30.4, pp. 221–235. ISSN: 0267-7261. DOI: https://doi.org/10.1016/j.soildyn.2009.11.002 (cit. on p. 3).

Andersen, K. H. (1988). *Properties of Soft Clay under Static and Cyclic Loading*. Tech. rep. 176. Oslo, Norway: Norwegian Geotechnical Institute, p. 20 (cit. on p. 3).

Andersen, K. H. (2009). "Bearing capacity under cyclic loading — offshore, along the coast, and on land. The 21st Bjerrum Lecture presented in Oslo, 23 November 2007". In: *Canadian Geotechnical Journal* 46.5, pp. 513–535. DOI: 10.1139/T09-003. URL: https://doi.org/10.1139/T09-003 (cit. on pp. 3, 5).

Ansal, A. M. and Erken, A. (1989). "Undrained behavior of clay under cyclic shear stresses". In: *Journal of Geotechnical Engineering* 115.7, pp. 968–983 (cit. on p. 3).

Augustin, S., Gudehus, G., Huber, G., and Schünemann, A. (2003). "Numerical Model and Laboratory Tests on Settlement of Ballast Track". In: *System Dynamics and Long-Term Behaviour of Railway Vehicles, Track and Subgrade*. Ed. by K. Popp and W. Schiehlen. Berlin, Heidelberg: Springer Berlin Heidelberg, pp. 317–336 (cit. on p. 3).

Bian, X., Jiang, H., Cheng, C., Chen, Y., Chen, R., and Jiang, J. (2014). "Full-scale model testing on a ballastless high-speed railway under simulated train moving loads". In: *Soil Dynamics and Earthquake Engineering* 66, pp. 368–384. ISSN: 0267-7261. DOI: https://doi.org/10.1016/j.soildyn.2014.08.003 (cit. on p. 3).

Bishop, A. and Wesley, L. (1975). "A hydraulic triaxial apparatus for controlled stress path testing". In: *Géotechnique* 25.4, pp. 657–670 (cit. on p. 27).

Box, G. E. P. and Draper, N. R. (1987). *Empirical Model-Building and Response Surfaces*. Wiley Series in Probability and Statistics. Wiley. ISBN: 0-471-81033-9 (cit. on p. 15).

Box, G. E. P., Hunter, J. S., and Hunter, W. G. (2009). *Statistics for Experimenters; Design, Innovation, and Discovery*. Hoboken, New Jersey: John Wiley & Sons, Inc., pp. 1–655. ISBN: 978-0-471-71813-0 (cit. on pp. 1, 13, 20, 21).

Buisman, A. S. K. (1936). "Results of Long Duration Settlement Tests". In: *Proceedings, 1st International Conference on Soil Mechanics and Foundation Engineering*. Vol I. Cambridge Massachusetts, US: Harvard University, pp. 103–106 (cit. on p. 4).

Burland, J. B. (1989). "Ninth Laurits Bjerrum Memorial Lecture: "Small is beautiful"—the stiffness of soils at small strains". In: *Canadian Geotechnical Journal* 26.4, pp. 499–516. DOI: 10.1139/t89-064 (cit. on p. 6).

Cacuci, D. G. (2003). *Sensitivity & Uncertainty Analysis, Volume I: Theory*. New York, US: Chapman and Hall/CRC (cit. on p. 17).

Cui, X., Zhang, N., Li, S., Zhang, J., and Wang, L. (2015). "Effects of embankment height and vehicle loads on traffic-load-induced cumulative settlement of soft clay subsoil". In: *Arabian Journal of Geosciences* 8, pp. 2487–2496 (cit. on p. 3).

Czitrom, V. (1999). "One-Factor-at-a-Time Versus Designed Experiments". In: *The American Statistician* 53.2, pp. 126–131 (cit. on pp. 15, 20).

Dafalias, Y. F., Manzari, M. T., and Papadimitriou, A. G. (2006). "SANICLAY: simple anisotropic clay plasticity model". In: *International Journal for Numerical and Analytical Methods in Geomechanics* 30.12, pp. 1231–1257 (cit. on p. 1).

Daniel, C. (1973). "One-at-a-Time Plans". In: *Journal of the American Statistical Association* 68.342, pp. 353–360. DOI: 10.1080/01621459.1973.10482433 (cit. on p. 20).

Daniel, C. (1976). *Applications of Statistics to Industrial Experimentation*. Wiley Series in Probability and Statistics. Wiley. ISBN: 9780471194699 (cit. on p. 20).

Darendeli, M. B. (2001). "Development of a new family of normalized modulus reduction and material damping curves". PhD thesis. The university of Texas at Austin (cit. on pp. 6, 24).

Dijkstra, J., Tahershamsi, H., and Ahmadi-Naghadeh, R. (2022). *Degradation of a natural sensitive clay under cyclic loading*. Tech. rep. Chalmers University of Technology, Sweden (cit. on pp. 26, 27).

Einstein, H. H. and Baecher, G. B. (1983). "Probabilistic and statistical methods in engineering geology". In: *Rock mechanics and rock engineering* 16.1, pp. 39–72 (cit. on p. 13).

Esveld, C. (2001). *Modern Railway Track*. 2nd ed. The Netherlands: MRT-Productions. ISBN: 90-800324-3-3 (cit. on p. 3).

Fang, Y. and Su, Y. (2020). "On the use of the global sensitivity analysis in the reliability-based design: Insights from a tunnel support case". In: *Computers and Geotechnics* 117. ISSN: 18737633. DOI: 10.1016/j.compgeo.2019.103280. URL: https://doi.org/10.1016/j.compgeo.2019.103280 (cit. on pp. 13, 14).

Fenton, G. A. and Griffiths, D. V. (1993). "Statistics of Block Conductivity Through a Simple Bounded Stochastic Medium". In: *Water Resources Research* 29.6, pp. 1825–1830 (cit. on p. 13).

Fenton, G. A. and Griffiths, D. V. (2002). "Probabilistic Foundation Settlement on Spatially Random Soil". In: *Journal of Geotechnical and Geoenvironmental Engineering* 128.5, pp. 381–390. DOI: 10.1061/(ASCE)1090-0241(2002)128:5(381) (cit. on p. 13).

Fenton, G. A. and Vanmarcke, E. H. (1990). "Simulation of Random Fields via Local Average Subdivision". In: *Journal of Engineering Mechanics* 116.8, pp. 1733–1749 (cit. on p. 13).

Fisher, R. A. (1942). *The Design of Experiments*. Tweeddale Court, Edinburgh, UK: Oliver and Boyd Ltd., pp. 1–236 (cit. on p. 20).

François, S., Karg, C., Haegeman, W., and Degrande, G. (2010). "A numerical model for foundation settlements due to deformation accumulation in granular soils under repeated small amplitude dynamic loading". In: *International Journal for Numerical and Analytical Methods in Geomechanics* 34.3, pp. 273–296. DOI: https://doi.org/10.1002/nag.807. URL: https://onlinelibrary.wiley.com/doi/abs/10.1002/nag.807 (cit. on p. 11).

Graham, J., Crooks, J. H. A., and Bell, A. L. (1983). "Time effects on the stress-strain behaviour of natural soft clays". In: *Géotechnique* 33.3, pp. 327–340. DOI: 10.1680/geot.1983.33.3.327. URL: https://doi.org/10.1680/geot.1983.33.3.327 (cit. on p. 4).

Gras, J.-P., Sivasithamparam, N., Karstunen, M., and Dijkstra, J. (2017). "Strategy for consistent model parameter calibration for soft soils using multi-objective optimisation". In: *Computers and Geotechnics* 90, pp. 164–175. ISSN: 0266352X (cit. on pp. 1, 9).

Gras, J.-P., Sivasithamparam, N., Karstunen, M., and Dijkstra, J. (2018). "Permissible range of model parameters for natural fine-grained materials". In: *Acta Geotechnica*. ISSN: 18611133 (cit. on pp. 1, 4, 7, 8, 23).

Griffiths, D. V. and Fenton, G. A. (1993). "Seepage beneath water retaining structures founded on spatially random soil". In: *Geotechnique* 43.4, pp. 577–587. ISSN: 17517656. DOI: 10.1680/geot.1993.43.4.577 (cit. on p. 13).

Grimstad, G., Degago, S. A., Nordal, S., and Karstunen, M. (2010). "Modeling creep and rate effects in structured anisotropic soft clays". In: *Acta Geotechnica* 5.1, pp. 69–81 (cit. on pp. 4, 24).

Guler, H., Jovanovic, S., and Evren, G. (2011). "Modelling railway track geometry deterioration". In: *Proceedings of the Institution of Civil Engineers - Transport* 164.2, pp. 65–75. DOI: 10.1680/tran.2011.164.2.65 (cit. on p. 3).

Hall, L. (2003). "Simulations and analyses of train-induced ground vibrations in finite element models". In: *Soil Dynamics and Earthquake Engineering* 23.5, pp. 403–413. ISSN: 0267-7261. DOI: https://doi.org/10.1016/S0267-7261(02)00209-9 (cit. on p. 3).

Hardin, B. O. and Drnevich, V. P. (1972). "Shear modulus and damping in soils: design equations and curves". In: *Journal of the Soil mechanics and Foundations Division* 98.7, pp. 667–692 (cit. on pp. 6, 24).

Herman, J. and Usher, W. (2017). "SALib: An open-source Python library for Sensitivity Analysis". In: *The Journal of Open Source Software* 2.9. DOI: 10.21105/joss.00097. URL: https://doi.org/10.21105/joss.00097 (cit. on p. 29).

Holm, G., Andreasson, B., Bengtsson, P., Bodare, A., and Eriksson, H. (2002). *Mitigation of Track and Ground Vibrations bu High Speed Trains at Ledsgård, Sweden*. Tech. rep. Report 10. Linköping, Sweden: Swedish Deep Stabilization Research Centre, p. 60 (cit. on p. 3).

Homma, T. and Saltelli, A. (1996). "Importance measures in global sensitivity analysis of model output". In: *Reliability Engineering and System Safety* 52, pp. 1–17. ISSN: 0951-8320 (cit. on p. 18).

Indraratna, B., Ionescu, D., and Christie, H. D. (1998). "Shear Behavior of Railway Ballast Based on Large-Scale Triaxial Tests". In: *Journal of Geotechnical and Geoenvironmental Engineering* 124.5, pp. 439–449. DOI: 10.1061/(ASCE)1090-0241(1998)124:5(439) (cit. on p. 3).

Indraratna, B. and Salim, W. (2002). "Modelling of particle breakage of coarse aggregates incorporating strength and dilatancy". In: *Proceedings of the Institution of Civil Engineers - Geotechnical Engineering* 155.4, pp. 243–252. DOI: 10.1680/geng.2002.155.4.243. URL: https://doi.org/10.1680/geng.2002.155.4.243 (cit. on p. 3).

Indraratna, B., Thakur, P. K., Vinod, J. S., and Salim, W. (2012). "Semiempirical Cyclic Densification Model for Ballast Incorporating Particle Breakage". In: *International Journal of Geomechanics* 12.3, pp. 260–271. DOI: 10.1061/(ASCE)GM.1943-5622.0000135 (cit. on p. 3).

Janbu, N. (1969). "The resistance concept applied to deformations of soils". In: *Proceedings of the 7th international conference on soil mechanics and foundation engineering,* 1. Mexico city, pp. 191–196 (cit. on p. 22).

Janbu, N. (1976). "Soils under cyclic loading". In: *Proceedings of the first international conference BOSS'76*, pp. 373–385 (cit. on pp. 22, 23, 34).

Janbu, N. (1985). "Soil models in offshore engineering". In: *Géotechnique* 35.3, pp. 241–281. DOI: 10.1680/geot.1985.35.3.241. URL: https://doi.org/10.1680/geot.1985.35.3.241 (cit. on pp. 4, 5).

Jardine, R. J., Potts, D. M., Fourie, A. B., and Burland, J. B. (1986). "Studies of the influence of non-linear stress–strain characteristics in soil–structure interaction". In: *Géotechnique* 36.3, pp. 377–396. DOI: 10.1680/geot.1986.36.3.377 (cit. on p. 6).

Karlsson, M., Emdal, A., and Dijkstra, J. (2016). "Consequences of sample disturbance when predicting long-term settlements in soft clay". In: *Canadian Geotechnical Journal* 53.12, pp. 1965–1977. DOI: 10.1139/cgj-2016-0129. URL: https://doi.org/10.1139/cgj-2016-0129 (cit. on p. 4).

Karstunen, M., Krenn, H., Wheeler, S. J., Koskinen, M., and Zentar, R. (2005). "Effect of Anisotropy and Destructuration on the Behavior of Murro Test Embankment". In: *International Journal of Geomechanics* 5.2, pp. 87–97 (cit. on pp. 1, 7, 10).

Khaledi, K., Mahmoudi, E., Datcheva, M., König, D., and Schanz, T. (2016). "Sensitivity analysis and parameter identification of a time dependent constitutive model for rock salt". In: *Journal of Computational and Applied Mathematics* 293, pp. 128–138. ISSN: 0377-0427. DOI: https://doi.org/10.1016/j.cam.2015.03.049. URL: https://www.sciencedirect.com/science/article/pii/S0377042715002022 (cit. on p. 13).

Krylov, V. V., Dawson, A. R., Heelis, M. E., and Collop, A. C. (2000). "Rail movement and ground waves caused by high-speed trains approaching track-soil critical velocities". In: *Proceedings of the Institution of Mechanical Engineers, Part F: Journal of Rail and Rapid Transit* 214.2, pp. 107–116. DOI: 10.1243/0954409001531379. URL: https://doi.org/10.1243/0954409001531379 (cit. on p. 3).

Lefebvre, G. and LeBoeuf, D. (1987). "Rate Effects And Cyclic Loading of Sensitive Clays". In: *Journal of Geotechnical Engineering* 113.5, pp. 476–489. DOI: 10.1061/(ASCE)0733-9410(1987)113:5(476) (cit. on p. 5).

Leroueil, S., Kabbaj, M., Tavenas, F., and Bouchard, R. (1985). "Stress–strain–strain rate relation for the compressibility of sensitive natural clays". In: *Géotechnique* 35.2, pp. 159–180. DOI: 10.1680/geot.1985.35.2.159. URL: https://doi.org/10.1680/geot.1985.35.2.159 (cit. on p. 4).

Li, L.-L., Dan, H.-B., and Wang, L.-Z. (2011). "Undrained behavior of natural marine clay under cyclic loading". In: *Ocean Engineering* 38.16, pp. 1792–1805. ISSN: 0029-8018. DOI: https://doi.org/10.1016/j.oceaneng.2011.09.004. URL: https://www.sciencedirect.com/science/article/pii/S0029801811001983 (cit. on p. 5).

Li, X., Ekh, M., and Nielsen, J. C. O. (2016). "Three-dimensional modelling of differential railway track settlement using a cycle domain constitutive model". In: *International Journal for Numerical and Analytical Methods in Geomechanics* 40.12, pp. 1758–1770. DOI: https://doi.org/10.1002/nag.2515 (cit. on p. 3).

Li, Y., Dijkstra, J., and Karstunen, M. (2018). "Thermomechanical Creep in Sensitive Clays". In: *Journal of Geotechnical and Geoenvironmental Engineering* 144.11, p. 04018085. DOI: 10.1061/(ASCE)GT.1943-5606.0001965. URL: https://ascelibrary.org/doi/abs/10.1061/%28ASCE%29GT.1943-5606.0001965 (cit. on p. 4).

Liu, W., Wu, X., Zhang, L., Zheng, J., and Teng, J. (2017). "Global Sensitivity Analysis of Tunnel-Induced Building Movements by a Precise Metamodel". In: *Journal of Computing in Civil Engineering* 31.5. ISSN: 0887-3801. DOI: 10.1061/(asce)cp.1943-5487.0000681 (cit. on p. 13).

Madshus, C. and Kaynia, A. M. (2000). "High-speed railwat lines on soft ground: dynamic behaviour at critical train speed". In: *Journal of Sound and Vibration* 231.3, pp. 689–701. ISSN: 0022-460X. DOI: https://doi.org/10.1006/jsvi.1999.2647 (cit. on p. 3).

Mahmoudi, E., Hölter, R., Georgieva, R., König, M., and Schanz, T. (2019). "On the Global Sensitivity Analysis Methods in Geotechnical Engineering: A Comparative Study on a Rock Salt Energy Storage". In: *International Journal of Civil Engineering* 17.1, pp. 131–143. ISSN: 23833874. DOI: 10.1007/s40999-018-0302-3. URL: http://dx.doi.org/10.1007/s40999-018-0302-3 (cit. on p. 13).

Masurier, J. L., Blockley, D., and Muir Wood, D. (2006). "An observational model for managing risk". In: *Proceedings of the Institution of Civil Engineers - Civil Engineering* 159.6, pp. 35–40. DOI: 10.1680/cien.2006.159.6.35. URL: https://doi.org/10.1680/cien.2006.159.6.35 (cit. on p. 13).

Miro, S., Hartmann, D., and Schanz, T. (2014). "Global sensitivity analysis for subsoil parameter estimation in mechanized tunneling". In: *Computers and Geotechnics* 56, pp. 80–88. ISSN: 0266352X. DOI: 10.1016/j.compgeo.2013.11.003. URL: http://dx.doi.org/10.1016/j.compgeo.2013.11.003 (cit. on p. 13).

Mitchell, J. K. (1964). "Shearing Resistance of Soils as a Rate Process". In: *Journal of the Soil Mechanics and Foundations Division* 90.1, pp. 29–61. DOI: 10.1061/JSFEAQ.0000593. URL: https://ascelibrary.org/doi/abs/10.1061/JSFEAQ.0000593 (cit. on p. 4).

Mitchell, J. K. and Soga, K. (2005). *Fundamentals of Soil Behavior*. 3rd ed. Hoboken, New Jersey: John Wiley & Sons (cit. on p. 1).

Montgomery, D. C. (2009). *Design and analysis of experiments*. 7th ed. Hoboken, New Jersey: John Wiley and sons, p. 656. ISBN: 978-0-470-39882-1 (cit. on p. 21).

Morris, M. D. (1991). "Factorial Sampling Plans for Preliminary Computational Experiments". In: *Technometrics* 33.2, pp. 161–174. ISSN: 00401706. URL: http://www.jstor.org/stable/1269043 (cit. on p. 17).

Muir Wood, D. (2016). "Analysis of consolidation with constant rate of displacement". In: *Canadian Geotechnical Journal* 53.5, pp. 740–752 (cit. on p. 4).

Nielsen, J. C. and Li, X. (2018). "Railway track geometry degradation due to differential settlement of ballast/subgrade – Numerical prediction by an iterative procedure". In: *Journal of Sound and Vibration* 412, pp. 441–456. ISSN: 0022-460X. DOI: https://doi.org/10.1016/j.jsv.2017.10.005 (cit. on p. 3).

Niemunis, A., Wichtmann, T., and Triantafyllidis, T. (2005). "A high-cycle accumulation model for sand". In: *Computers and Geotechnics* 32.4, pp. 245–263. ISSN: 0266-352X. DOI: https://doi.org/10.1016/j.compgeo.2005.03.002 (cit. on p. 11).

Pasten, C., Shin, H., and Santamarina, J. C. (2014). "Long-Term Foundation Response to Repetitive Loading". In: *Journal of Geotechnical and Geoenvironmental Engineering* 140.4, p. 04013036. DOI: 10.1061/(ASCE)GT.1943-5606.0001052 (cit. on p. 11).

Peck, R. B. (1969). "Advantages and Limitations of the Observational Method in Applied Soil Mechanics". In: *Géotechnique* 19.2, pp. 171–187. DOI: 10.1680/geot.1969.19.2.171. URL: https://doi.org/10.1680/geot.1969.19.2.171 (cit. on p. 13).

Peck, R. B., Hanson, W. E., and Thornburn, T. H. (1974). *Foundation Engineering*. Hoboken, New Jersey: John Wiley & Sons, Inc. (cit. on p. 30).

Phoon, K.-K. (2020). "The story of statistics in geotechnical engineering". In: *Georisk: Assessment and Management of Risk for Engineered Systems and Geohazards* 14.1, pp. 3–25. DOI: 10.

1080/17499518.2019.1700423. eprint: https://doi.org/10.1080/17499518.2019.1700423. URL: https://doi.org/10.1080/17499518.2019.1700423 (cit. on p. 13).
Phoon, K.-K. and Kulhawy, F. H. (1999a). "Characterization of geotechnical variability". In: *Canadian Geotechnical Journal* 36.4, pp. 612–624. DOI: 10.1139/t99-038. eprint: https://doi.org/10.1139/t99-038. URL: https://doi.org/10.1139/t99-038 (cit. on p. 13).
Phoon, K.-K. and Kulhawy, F. H. (1999b). "Evaluation of geotechnical property variability". In: *Canadian Geotechnical Journal* 36.4, pp. 625–639. DOI: 10.1139/t99-039. eprint: https://doi.org/10.1139/t99-039. URL: https://doi.org/10.1139/t99-039 (cit. on p. 13).
Randolph, M. and Gourvenec, S. (2017). *Offshore geotechnical engineering*. CRC press (cit. on p. 3).
Roscoe, K. H. and Burland, J. B. (1968). "On the generalised stress-strain behaviour of wet clay". In: *Engineering plasticity*, pp. 535–609 (cit. on p. 7).
Rowe, R. K. and Hinchberger, S. D. (1998). "The significance of rate effects in modelling the Sackville test embankment". In: *Canadian Geotechnical Journal* 35.3, pp. 500–516. DOI: 10.1139/t98-021. URL: https://doi.org/10.1139/t98-021 (cit. on p. 4).
Salim, W. and Indraratna, B. (2004). "A new elastoplastic constitutive model for coarse granular aggregates incorporating particle breakage". In: *Canadian Geotechnical Journal* 41.4, pp. 657–671. DOI: 10.1139/t04-025. URL: https://doi.org/10.1139/t04-025 (cit. on p. 3).
Sällfors, G. (1975). "Preconsolidation pressure of soft, high-plastic clays." PhD thesis. Chalmers University of Technology. ISBN: 0346-718X (cit. on p. 4).
Saltelli, A., Tarantola, S., and Campolongo, F. (2000). "Sensitivity Analysis as an Ingredient of Modeling". In: *Statistical Science* 15.4, pp. 377–395. ISSN: 08834237. URL: http://www.jstor.org/stable/2676831 (cit. on p. 18).
Saltelli, A. (2002). "Making best use of model evaluations to compute sensitivity indices". In: *Computer Physics Communications* 145.2, pp. 280–297. ISSN: 00104655. DOI: 10.1016/S0010-4655(02)00280-1 (cit. on p. 19).
Saltelli, A. and Annoni, P. (2010). "How to avoid a perfunctory sensitivity analysis". In: *Environmental Modelling and Software* 25.12, pp. 1508–1517. ISSN: 1364-8152. DOI: 10.1016/j.envsoft.2010.04.012. URL: http://dx.doi.org/10.1016/j.envsoft.2010.04.012 (cit. on pp. 15, 20).
Saltelli, A., Annoni, P., Azzini, I., Campolongo, F., Ratto, M., and Tarantola, S. (2010). "Variance based sensitivity analysis of model output . Design and estimator for the total sensitivity index". In: *Computer Physics Communications* 181.2, pp. 259–270. ISSN: 0010-4655. DOI: 10.1016/j.cpc.2009.09.018. URL: http://dx.doi.org/10.1016/j.cpc.2009.09.018 (cit. on p. 19).
Saltelli, A., Ratto, M., Andres, T., Campolongo, F., Cariboni, J., Gatelli, D., Saisana, M., and Tarantola, S. (2008). *Global Sensitivity Analysis: The Primer*. Chichester, UK: John Wiley & Sons, Ltd, p. 312. ISBN: 978-0-470-05997-5 (cit. on pp. 13, 17, 19).
Sangrey, D., Henkel, D., and Esrig, M. (1969). "The effective stress response of a saturated clay soil to repeated loading". In: *Canadian Geotechnical Journal* 6.3, pp. 241–252 (cit. on p. 3).
Selig, E. T. and Waters, J. M. (1994). *Track geotechnology and substructure management*. Thomas Telford (cit. on p. 3).

SGF (2009). *Metodbeskrivning för provtagning med standardkolvprovtagare - ostörd provtagning i finkornig jord*. Tech. rep. 1. Stockholm: Swedish Geotechnical Society (cit. on p. 26).

Shih, J., Thompson, D., and Zervos, A. (2017). "The influence of soil nonlinear properties on the track/ground vibration induced by trains running on soft ground". In: *Transportation Geotechnics* 11, pp. 1–16. ISSN: 2214-3912. DOI: https://doi.org/10.1016/j.trgeo.2017.03.001 (cit. on p. 3).

Sivasithamparam, N., D'Ignazio, M., Tsegaye, A., Castro, J., and Madshus, C. (2021). "Small strain stiffness within logarithmic contractancy model for structured anisotropic clay". In: *IOP Conference Series: Earth and Environmental Science*. Vol. 710. 1. IOP Publishing, p. 012042 (cit. on p. 24).

Sivasithamparam, N., Karstunen, M., and Bonnier, P. (2015). "Modelling creep behaviour of anisotropic soft soils". In: *Computers and Geotechnics* 69, pp. 46–57. ISSN: 18737633. DOI: 10.1016/j.compgeo.2015.04.015. URL: http://dx.doi.org/10.1016/j.compgeo.2015.04.015 (cit. on pp. 4, 7–9).

Sobol', I. M. (1993). "Sensitivity Estimates for Nonlinear Mathematical Models". In: *MMCE (English translation from Russian paper)* 1, pp. 407–414 (cit. on pp. 18, 19).

Sobol', I. M. (2001). "Global sensitivity indices for nonlinear mathematical models and their Monte Carlo estimates". In: *Mathematics and Computers in Simulation* 55, pp. 271–280 (cit. on p. 18).

Spross, J. and Johansson, F. (2017). "When is the observational method in geotechnical engineering favourable?" In: *Structural Safety* 66, pp. 17–26. ISSN: 0167-4730. DOI: https://doi.org/10.1016/j.strusafe.2017.01.006 (cit. on p. 13).

Staubach, P., Machaček, J., Tafili, M., and Wichtmann, T. (2022). "A high-cycle accumulation model for clay and its application to monopile foundations". In: *Acta Geotechnica* 17.3, pp. 677–698 (cit. on pp. 1, 11).

Suiker, A. S. J. and Borst, R. de (2003). "A numerical model for the cyclic deterioration of railway tracks". In: *International Journal for Numerical Methods in Engineering* 57.4, pp. 441–470. DOI: https://doi.org/10.1002/nme.683. URL: https://onlinelibrary.wiley.com/doi/abs/10.1002/nme.683 (cit. on pp. 3, 11).

Suiker, A. S. J., Selig, E. T., and Frenkel, R. (2005). "Static and Cyclic Triaxial Testing of Ballast and Subballast". In: *Journal of Geotechnical and Geoenvironmental Engineering* 131.6, pp. 771–782. DOI: 10.1061/(ASCE)1090-0241(2005)131:6(771) (cit. on p. 3).

Tahershamsi, H., Ahmadi Naghadeh, R., Zuada Coelho, B., and Dijkstra, J. (2023). "Low amplitude strain accumulation model for natural soft clays below railways". In: *Submitted to Transportation Geotechnics* (cit. on pp. 31, 77).

Tahershamsi, H. and Dijkstra, J. (2021). "Towards rigorous boundary value level sensitivity analyses using FEM". In: *IOP Conference Series: Earth and Environmental Science* 710.1, p. 012072. DOI: 10.1088/1755-1315/710/1/012072. URL: https://doi.org/10.1088/1755-1315/710/1/012072 (cit. on pp. 29, 47).

Tahershamsi, H. and Dijkstra, J. (2022). "Using experimental design to assess rate-dependent numerical models". In: *Soils and Foundations* 62.6, p. 101244. ISSN: 0038-0806. DOI: https://doi.org/10.1016/j.sandf.2022.101244 (cit. on pp. 30, 59).

Tang, W. H., Yucemen, M. S., and Ang, A. H.-S. (1976). "Probability-based short term design of soil slopes". In: *Canadian Geotechnical Journal* 13.3, pp. 201–215. DOI: 10.1139/t76-024.

eprint: https://doi.org/10.1139/t76-024. URL: https://doi.org/10.1139/t76-024 (cit. on p. 13).

Tavenas, F. and Leroueil, S. (1977). "Effects of Stresses and Time on Yielding of Clays". In: *Proceedings, 9th International Conference on Soil Mechanics and Foundation Engineering*. Vol I. Tokyo, Japan, pp. 319–326 (cit. on p. 4).

Tavenas, F., Leroueil, S., Rochelle, P. L., and Roy, M. (1978). "Creep behaviour of an undisturbed lightly overconsolidated clay". In: *Canadian Geotechnical Journal* 15.3, pp. 402–423. DOI: 10.1139/t78-037. URL: https://doi.org/10.1139/t78-037 (cit. on p. 4).

Tochnog Professional (n.d.). *Tochnog Professional, Free Finite Element Software*. URL: https://www.tochnogprofessional.nl (cit. on p. 29).

Wheeler, S., Näätänen, A., Karstunen, M., and Lojander, M. (2003). "An anisotropic elastoplastic model for soft clays". In: *Canadian Geotechnical Journal* 40.2, pp. 403–418. DOI: 10.1139/t02-119 (cit. on pp. 1, 7, 10).

Wichtmann, T., Andersen, K., Sjursen, M., and Berre, T. (2013). "Cyclic tests on high-quality undisturbed block samples of soft marine Norwegian clay". In: *Canadian Geotechnical Journal* 50.4, pp. 400–412. DOI: 10.1139/cgj-2011-0390. eprint: https://doi.org/10.1139/cgj-2011-0390. URL: https://doi.org/10.1139/cgj-2011-0390 (cit. on pp. 5, 6, 12).

Wichtmann, T. (2005). "Explicit accumulation model for non-cohesive soils under cyclic loading". PhD thesis. Ruhr-Universit Bochum (cit. on p. 11).

Wood, T. (2016). "On the Small Strain Stiffness of Some Scandinavian Soft Clays and Impact on Deep Excavations". PhD thesis. Chalmers University of Technology (cit. on pp. 7, 26).

Woodward, P. K., Laghrouche, O., Mezher, S. B., and Connolly, D. (2015). "Application of coupled train-track modelling of critical speeds for high-speed trains using three-dimensional non-linear finite elements". In: *International Journal of Railway Technology* 4.3, pp. 1–35 (cit. on p. 3).

Yildiz, A. and Uysal, F. (2016). "Modelling of anisotropy and consolidation effect on behaviour of sunshine embankment: Australia". In: *International Journal of Civil Engineering* 14.2, pp. 83–95 (cit. on p. 4).

Yin, Z.-Y., Chang, C. S., Karstunen, M., and Hicher, P.-Y. (2010). "An anisotropic elastic–viscoplastic model for soft clays". In: *International Journal of Solids and Structures* 47.5, pp. 665–677. ISSN: 0020-7683. DOI: https://doi.org/10.1016/j.ijsolstr.2009.11.004 (cit. on p. 4).

Zhao, C., Lavasan, A. A., Hölter, R., and Schanz, T. (2018). "Mechanized tunneling induced building settlements and design of optimal monitoring strategies based on sensitivity field". In: *Computers and Geotechnics* 97, pp. 246–260. ISSN: 18737633. DOI: 10.1016/j.compgeo.2018.01.007. URL: https://doi.org/10.1016/j.compgeo.2018.01.007 (cit. on p. 13).

Zhao, C., Liu, J., Liu, H., Bian, X., and Chen, Y. (2023). "A conceptual model for the shakedown response of soft clay to high-cycle, low-amplitude undrained loading". In: *Computers and Geotechnics* 156, p. 105257 (cit. on p. 3).

Zuada Coelho, B., Dijkstra, J., and Karstunen, M. (2021). "Viscoplastic cyclic degradation model for soft natural soils". In: *Computers and Geotechnics* 135, p. 104176 (cit. on pp. 1, 4, 11, 34).

Table 4.2: General overview of triaxial tests for Kärra clay.

Test#	AC[i]	C1[ii]	PS[iii]	C2[iv]	CL[v]	test duration	p'_0	q_0	q_p	q_m	q_{cyc}	q_{cyc}/p'_0	Cyclic failure
-	day, d	day, d	day, d	day, d	day, d	day, d	kPa	kPa	kPa	kPa	kPa	-	-
Test04	1.00	5.10	0.01	13.73	31.25	16.98	53.83	28.00	19.00	47.00	5	0.09	No
Test05	1.00	5.10	0.00	0.00	30.74	36.84	49.53	28.00	0.00	28.00	5	0.10	No
Test06	1.00	0.72	0.00	0.00	57.09	58.81	51.03	29.80	0.00	29.80	10	0.20	No
Test07	0.83	7.10	0.00	0.00	100.97	108.90	55.70	29.10	0.00	29.10	20	0.36	Yes
Test08	1.00	2.93	0.01	13.90	1.26	19.10	53.10	28.50	9.00	37.70	20	0.38	Yes
Test09	1.00	0.89	0.00	0.00	12.18	14.07	52.63	28.30	0.00	28.30	28	0.53	Yes
Test10	1.00	2.70	0.04	7.00	20.90	31.64	52.30	28.60	-18.00	10.30	29	0.53	Yes
Test11	1.00	5.10	0.01	13.78	0.19	20.08	49.60	27.90	-8.00	20.30	38	0.77	Yes

[i] AC = Anisotropic Consolidation [ii] C1 = Creep 1 [iii] PS = Pre-shearing [iv] C2 = Creep 2 [v] CL = Cyclic Loading